สมบัติเชิงเส้นกำกับของแบบจำลองการเติบโตของฟิล์มบางด้วยวิธีการแจกแจงความขรุขระโดยใช้และไม่ใช้เทคนิคการลดสิ่งรบกวน

นางปราณี ดิษรัฐกิจ

วิทยานิพนธ์นี้เป็นส่วนหนึ่งของการศึกษาตามหลักสูตรปริญญาวิทยาศาสตรดุษฎีบัณฑิต
สาขาวิชาฟิสิกส์ ภาควิชาฟิสิกส์
คณะวิทยาศาสตร์ จุฬาลงกรณ์มหาวิทยาลัย
ปีการศึกษา 2558

ASYMPTOTIC PROPERTIES OF THIN FILM GROWTH MODELS THROUGH THE ROUGHNESS DISTRIBUTION METHOD WITH AND WITHOUT NOISE REDUCTION TECHNIQUES

Mrs. Pranee Disrattakit

A Dissertation Submitted in Partial Fulfillment of the Requirements
for the Degree of Doctor of Philosophy Program in Physics
Department of Physics
Faculty of Science
Chulalongkorn University
Academic Year 2015

Thesis Title	ASYMPTOTIC PROPERTIES OF THIN FILM GROWTH MODELS THROUGH THE ROUGHNESS DISTRIBUTION METHOD WITH AND WITHOUT NOISE REDUCTION TECHNIQUES
By	Mrs. Pranee Disrattakit
Field of Study	Physics
Thesis Advisor	Assistant Professor Patcha Chatraphorn, Ph.D.

Accepted by the Faculty of Science, Chulalongkorn University in Partial Fulfillment of the Requirements for the Doctoral Degree

.....Dean of the Faculty of Science
(Associate Professor Polkit Sangvanich, Ph.D.)

THESIS COMMITTEE

.....Chairman
(Associate Professor Nakorn Phaisangittisakul, Ph.D.)
.....Thesis Advisor
(Assistant Professor Patcha Chatraphorn, Ph.D.)
.....Examiner
(Somrit Wongmanerod, Ph.D.)
.....Examiner
(Panadda Dechadilok, Ph.D.)
.....External Examiner
(Soontorn Chanyawadee, Ph.D.)

ปราณี ดิษรัฐกิจ : สมบัติเชิงเส้นกำกับของแบบจำลองการเติบโตของฟิล์มบางด้วยวิธีการแจกแจงความขรุขระโดยใช้และไม่ใช้เทคนิคการลดสิ่งรบกวน (ASYMPTOTIC PROPERTIES OF THIN FILM GROWTH MODELS THROUGH THE ROUGHNESS DISTRIBUTION METHOD WITH AND WITHOUT NOISE REDUCTION TECHNIQUES) อ.ที่ปรึกษาวิทยานิพนธ์หลัก: ผศ. ดร .ปัจฉา ฉัตราภรณ์, 84 หน้า.

การศึกษาที่ผ่านมา การหาสมบัติเชิงเส้นกำกับของแบบจำลองการเติบโตของฟิล์มบางจะใช้วิธีการพิจารณามาตราส่วนการแกว่งของค่าเบี่ยงเบนมาตรฐานของผิวฟิล์ม ซึ่งวิธีนี้ต้องใช้การสร้างสถานการณ์จำลอง บนแผ่นรองรับขนาดใหญ่เพื่อลดผลกระทบของขนาดแผ่นรองรับที่จำลองได้ในขนาดจำกัด จึงได้มีการนำเทคนิคการลดสิ่งรบกวนที่เรียกว่า การตกซ้ำ (multiple hit) และเทคนิคการลดสิ่งรบกวนที่เรียกว่า การเพิ่มระยะการแพร่บนพื้นผิวมาช่วยหาสมบัติเชิงเส้นกำกับของแบบจำลองการเติบโตของฟิล์มบาง ต่อมามีการเสนอวิธีทางเลือกใหม่ ซึ่งเป็นวิธีที่เกี่ยวข้องกับการเปรียบเทียบการแจกแจงความขรุขระ ในสภาวะที่การแกว่งของค่าเบี่ยงเบนมาตรฐานของผิวฟิล์มมีค่าคงที่ ซึ่งเรียกว่าสถานะคงตัว ในการศึกษาครั้งนี้ ส่วนแรกทำการคำนวณการแจกแจงความขรุขระของแบบจำลองการเติบโตของฟิล์มบางตามแบบจำลอง ballistic deposition (BD) Das Sarma-Tamborenea (DT) Wolf-Villain (WV) Larger curvature model (LC) และ Family (F) ในระบบ (2+1) มิติ โดยไม่ใช้เทคนิคการลดสิ่งรบกวน จากนั้นทำการหาการแจกแจงความขรุขระของแบบจำลอง DT WV และ LC ที่ใช้เทคนิคการลดสิ่งรบกวนทั้งสองแบบ เพื่อศึกษาอิทธิพลของเทคนิคการลดสิ่งรบกวนต่อการแจกแจงความขรุขระ ผลการศึกษาแสดงให้เห็นว่า ในสภาวะสถานะคงตัว เทคนิคการลดสิ่งรบกวนทั้งสองแบบแทบจะไม่มีผลต่อการแจกแจงความขรุขระของฟิล์มที่เติบโตตามแบบจำลอง DT แต่ส่งผลมากต่อการแจกแจงความขรุขระของฟิล์มบางที่เติบโตตามแบบจำลอง LC และ WV โดยทำให้การแจกแจงความขรุขระเปลี่ยนเป็นการแจกแจงปกติอย่างมีนัยสำคัญ นอกจากนี้ยังพบว่า ขนาดแผ่นรองรับในการปลูกฟิล์มมีผลต่อการแจกแจงความขรุขระของผิวฟิล์มที่เติบโตตามแบบจำลอง DT LC และ WV ที่ใช้เทคนิคการลดสิ่งรบกวนน้อยมาก ส่วนที่สอง ทำการศึกษาผลกระทบของเทคนิคการลดสิ่งรบกวนต่อการแจกแจงความสูงของแบบจำลองการเติบโตของฟิล์มบางแบบ LC WV และ DT การบอกลักษณะเฉพาะของการแจกแจงความสูงของฟิล์มทำโดยการคำนวนค่าความเบ้ (skewness) และ เคอร์โทซีส (kurtosis) ผลการศึกษาพบว่า การแกว่งไกว (oscillation) ของความเบ้และเคอร์โทซีสเป็นลักษณะเฉพาะที่แสดงการเติบโตของฟิล์มแบบชั้นต่อชั้น ซึ่งเกิดขึ้นในช่วงแรกเริ่มของการปลูกฟิล์มตามแบบจำลอง LC WV และ DT ที่ใช้เทคนิคการลดสิ่งรบกวน สำหรับที่สภาวะสถานะคงตัว เทคนิคการลดสิ่งรบกวนทั้งสองแบบมีผลกระทบต่อการแจกแจงความสูงของการเติบโตของฟิล์มบางตามแบบจำลอง LC และ WV น้อยมาก ค่าความเบ้และเคอร์โทซีสของทั้งสองแบบจำลองมีค่าประมาณเท่ากัน แต่เทคนิคการลดสิ่งรบกวนมีผลกระทบต่อการแจกแจงความสูงของการเติบโตของฟิล์มบางตามแบบจำลอง DT อย่างมาก สุดท้ายพบว่า ขนาดแผ่นรองรับที่จำกัดมีผลต่อการแจกแจงความสูงของผิวฟิล์มบางที่เติบโตตามแบบจำลอง LC และ F น้อยมาก แต่มีผลต่อแบบจำลอง BD อย่างมาก

ภาควิชา ฟิสิกส์ ลายมือชื่อนิสิต .....

สาขาวิชา ฟิสิกส์ ลายมือชื่อ อ.ที่ปรึกษาหลัก .....

ปีการศึกษา 2558

5373813623 : MAJOR PHYSICS
KEYWORDS: ROUGHNESS DISTRIBUTION / HEIGHT DISTRIBUTION / ASYMPTOTIC PROPERTY / NOISED REDUCTION TECNIQUE / GROWTH MODEL

PRANEE DISRATTAKIT: ASYMPTOTIC PROPERTIES OF THIN FILM GROWTH MODELS THROUGH THE ROUGHNESS DISTRIBUTION METHOD WITH AND WITHOUT NOISE REDUCTION TECHNIQUES. ADVISOR: ASST. PROF. PATCHA CHATRAPHORN, Ph.D., 84 pp.

Conventionally, the asymptotic property of a growth model is identified via the scaling of interface width. This method requires large-scale simulations to minimize finite-size effects on the results. The multiple hit noise and the long surface diffusion length noise reduction techniques (NRTs) have been used to promote the asymptotic behaviors of the growth models. Lately, an alternative method involving comparison of roughness distribution in the steady state has been proposed. In this work, firstly, the roughness distribution of the (2+1)-dimensional ballistic deposition (BD), Das Sarma-Tamborenea (DT), Wolf-Villain (WV), Larger Curvature (LC), and Family (F) models, without the NRTs, are calculated. Next, the noise reduced DT, WV, and LC models are studied in order to investigate the effects of the NRTs on the roughness distributions. In the steady state, our results indicate that the NRTs do not seem to have any impact on the roughness distribution of the DT model, but it significantly changes the roughness distributions of the LC and WV models to the normal distribution curves. Furthermore, we found that the finite substrate size does not strongly affect the roughness distributions of the noise reduced DT, LC, and WV models. Secondly, the effects of the NRTs on the height distributions of the LC, WV, and DT models are also studied. Qualitative characterization of the height distributions can be done via skewness and kurtosis calculation. The result shown that oscillating skewness and kurtosis are characteristic of layer-by-layer growth mode at early growth time of the films grown with the noise reduced LC, WV, and DT models. In the steady state, both NRTs slightly affect the height distributions of the LC and WV models and their skewness and kurtosis are approximately the same. The NRTs have strong effect on the height distribution of the DT models at the steady state. Finally, we found that the finite size effects on the height distributions of the films grown with the LC and F models are very weak, but the finite substrate size does strongly affect the height distribution of the BD model.

Department: Physics
Field of Study: Physics
Academic Year: 2015

Student's Signature .....

Advisor's Signature .....

ACKNOWLEDGEMENTS

This thesis can be completed with the extensive support and assistance from my advisor, Asst. Prof. Dr. Patcha Chatraphorn. I am grateful to my advisor for her valuable advice and guidance on this work.

I wish to thank Asst. Prof. Dr. Sojiphong Chatraphorn for his guidance and for the facility such as high-efficiency computer. I wish to thank Asst. Prof. Dr. Kajornyod Yoodee, Dr. Chatchai Srinitiwarawong, Asst. Prof. Dr. Surachate Limkumnerd and Dr. Rangsima Chanphana for valuable suggestions.

I would like to thank the students in Semiconductor Physics Research Laboratory (SPRL) for all the help and ideas during this work. I would like to thank my thesis committee, Assoc. Prof. Dr. Nakorn Phaisangittisakul, Dr. Somrit Wongmanerod, Dr. Panadda Dechadilok, and Dr. Soontorn Chanyawadee. Their comments on this thesis are also greatly appreciated.

I would like to thank Mahidolwittayunusorn School for supporting a scholarship during my study. I wish to thank the staffs of Mahidolwittayanusorn School and especially thank the team of physics department for hard working when I am a graduate student.

Finally, I especially thank my family, my dear son and daughter, and my husband for love and everything. I also thank my mother, brother, father and mother-in-law for every supporting me.

CONTENTS

Page
THAI ABSTRACT iv
ENGLISH ABSTRACT v
ACKNOWLEDGEMENTS vi
CONTENTS vii
List of Table 1
Page 1
List of Figures 2
Page 2
CHAPTER I 5
INTRODUCTION 5
CHAPTER II 9
MODEL AND THEORY 9
2.1 Growth models and universality class 9
2.1.1 The BD, DT, WV, LC, and F models 9
2.1.2 Universality class of the Growth models 12
2.2 The Growth models with the NRTs 15
2.2.1 Multiple hit noise reduction technique 15
2.2.2 Long surface diffusion length noise reduction technique 17
2.3 Quantities of interest 18
2.3.1 Interface width 18
2.3.2 Roughness distribution 19
2.3.3 Height distribution 20
CHAPTER III 23
RESULTS AND DISCUSSIONS: SURFACE MORPHOLOGY AND INTERFACE WIDTH OF GROWTH MODELS 23
3.1 Surface morphologies of growth models with and without the NRTs 23
3.2 Effects of the NRTs on the interface width and the growth exponent 35

Page

3.2.1 Interface width of the DT, WV, and LC models with and without the NRTs 35
3.2.2 Effects of the NRTs on the growth exponent of the DT, WV, and LC models 40
CHAPTER IV 48
RESULTS AND DISCUSSIONS: ROUGHNESS DITRIBUTION 48
4.1 Roughness distributions of growth models without the NRTs 48
4.2 Roughness distributions of growth models with the NRTs 51
4.3 Effects of substrate size on the roughness distribution 53
CHAPTER V 59
RESULTS AND DISCUSSIONS: HEIGHT DISTRIBUTION 59
5.1 Skewness and kurtosis of the height distribution in the early time 59
5.1.1 The LC, DT, and WV models with the multiple hit NRT 59
5.1.2 The LC and DT models with the long surface diffusion length NRT 63
5.2 Skewness and kurtosis of the height distribution in the steady state 66
5.2.1 The LC, WV, and DT models with the multiple hit NRT 66
5.2.2 The LC, WV, and DT models with the long surface diffusion length NRT 71
5.3 Finite size effect on skewness and kurtosis of the height distribution at the steady state for the BD, LC, and F models. 74
CHAPTER VI 78
CONCLUSIONS 78
REFERENCES 82
VITA 84

List of Table

Page

Table 1 The values of S and Q for the BD, DT, WV, LC, and F models with and without NRTs. 58

List of Figures

Page

Fig. 2. 1 Diagrams illustrating diffusion rules of the (2+1)-dimensional (a) BD, (b) DT, (c) WV, (d) LC, and (c) F models. The adatom moves in the direction indicated by the arrows. 10

Fig. 2. 2 Illustrations of the *m* >1 NRT in the case that m = 3 on (2+1)-dimensional flat substrates. After deposited atom selects its final site, the counter of that site is increased by one but its height does not change until the counter is equal to 3. 16

Fig. 2. 3 Illustrations geometrical characteristics of the distribution according to the value of *S* 21

Fig. 2. 4 Illustrations geometrical characteristics of the distribution according to the value of *Q* 21

Fig. 3. 1 Surface morphologies of the BD model 25

Fig. 3. 2 Surface morphologies of the BD model with and without m>1 NRT. 26

Fig. 3. 3 Surface morphologies of the DT model with and without NRTs. 27

Fig. 3. 4 Surface morphologies of the WV model 28

Fig. 3. 5 Surface morphologies of the WV model with the m>1 NRT 29

Fig. 3. 6 Surface morphologies of the WV model with the long surface diffusion length NRT 31

Fig. 3. 7 Surface morphologies of the LC model 32

Fig. 3. 8 Surface morphologies of the LC model with the m>1 NRT 33

Fig. 3. 9 Surface morphologies of the LC model with the long surface diffusion length NRT 34

Fig. 3. 10 Surface morphologies of the F model with and without NRTs. 36

Fig. 3. 11 Plots of *W(t)* for the DT model with the m>1 NRT. 37

Fig. 3. 12 Plots of *W(t)* for the WV model with the m>1 NRT. 38

Fig. 3. 13 Plots of *W(t)* for the LC model with the m>1 NRT. 39

Fig. 3. 14 Plots of *W(t)* for the DT model with the long surface diffusion length NRT 41

Fig. 3. 15 Plots of *W(t)* for the WV model with the long surface diffusion length NRT.....42

Fig. 3. 16 Plots of *W(t)* for the LC model with the long surface diffusion length NRT.....43

Fig. 3. 17 Plots of growth exponent versus m for the DT (square), WV (triangle), and LC (circle) models.....44

Fig. 3. 18 Plots of growth exponent versus *l*/L for the DT (square), WV (triangle), and LC (circle) models.....44

Fig. 3. 19 Plots of efective growth exponent versus lonsurface diffusion parameter for the DT (square), WV (triangle), and LC (circle) models. 47

Fig. 3. 20 Plots of growth exponent versus l/L for the DT. 47

Fig. 4. 1 Roughness distribution of the BD model. 49

Fig. 4. 2 Roughness distribution of the DT model.....49

Fig. 4. 3 Roughness distribution of the WV model. 50

Fig. 4. 4 Roughness distribution of the LC model. 50

Fig. 4. 5 Roughness distribution of the F model. 51

Fig. 4. 6 Roughness distributions of the DT model with the m>1 NRT. 52

Fig. 4. 7 Roughness distributions of the DT model with the long surface diffusion length NRT.....52

Fig. 4. 8 Roughness distributions of the WV model with the m>1 NRT. 54

Fig. 4. 9 Roughness distributions of the WV model with the long surface diffusion length NRT.. 54

Fig. 4. 10 Roughness distributions of the LC model with the m>1 NRT. Solid line shows the fit obtained with the Gaussian function. 55

Fig. 4. 11 Roughness distributions of the LC model with the long surface diffusion length NRT.. 55

Fig. 4. 12 Roughness distributions of the (a) DT model, (b) WV model, and (c) LC model with the NRTs using various substrate sizes. 56

Fig. 5. 1 Plots of (a) *S* and (b) *Q* versus *t* at early growth time of the LC model with the m>1 NRT 60

Fig. 5. 2 Surface morphologies of the LC model when m=10; (a) at 0.5 ML (b) at 0.9 ML (c) at 1.0 ML, and (d) at 1.1 ML. 61

Fig. 5. 3 Plots of (a) *S* and (b) *Q* versus *t* at early growth time of the DT model with the m>1 NRT. 64

Fig. 5. 4 Plots of (a) *S* and (b) *Q* versus *t* at early growth time of the WV model with the m>1 NRT. 65

Fig. 5. 5 Plots of (a) *S* and (b) *Q* versus *t* at early growth time of the LC model with the long surface diffusion length NRT. 67

Fig. 5. 6 Plots of (a) *S* and (b) *Q* versus *t* at early growth time of the DT model with the long surface diffusion length NRT. 68

Fig. 5. 7 Surface morphologies of the m>1 LC model at the steady state with (a) m=1, (b) m=3, (c) m=5, and (d) m=10. 69

Fig. 5. 8 Plots of the height distribution at the steady state of the LC model with the m>1 NRT. 70

Fig. 5. 9 Plots of *S* and *Q* of the height distribution at the steady state of the LC model with the m>1 NRT. 70

Fig. 5. 10 Plots of *S* and *Q* of the height distribution at the steady state of the WV model with the m>1 NRT. 72

Fig. 5. 11 Plots of *S* and *Q* of the height distribution at the steady state of the DT model with the m>1 NRT. 72

Fig. 5. 12 Plots of *S* and *Q* at the steady state for the LC model with the long surface diffusion length NRT. 73

Fig. 5. 13 Plots of *S* and *Q* at the steady state for the WV model with the long surface diffusion length NRT. 73

Fig. 5. 14 Plots of *S* and *Q* at the steady state for the DT model with the long surface diffusion length NRT. 75

Fig. 5. 15 Plots of *S* and *Q* at the steady state versus $1/L$ of the BD model when L= 32, 64, 128, 256, and 512. 75

Fig. 5. 16 Plots of *S* and *Q* at the steady state versus $1/L^{0.2}$ of the LC model when L= 32, 64, 128, 256, and 512. 76

Fig. 5. 17 Plots of *S* and *Q* at the steady state versus $1/L$ of the F model when L= 32, 64, 128, 256, and 512. 77

CHAPTER I

INTRODUCTION

In thin film growth simulation, one of the interesting problems is to identify universality classes of discrete growth models. Determining the universality class is important because it helps us to identify the asymptotic behavior of a discrete growth model at very large scale, and to find a true continuum growth equation of a discrete growth model. Growth models that belong to the same universality class, have the same continuum growth equation. Simulating a very large substrate system is necessary to find a real universality class of a growth model, but it takes a long time. In addition, some growth models have crossover behaviors before a true asymptotic behavior can be seen. Examples include the solid-on-solid limited mobility discrete growth models such as the Das Sarma -Tamborenea (DT) model [1, 2] and the Wolf-Villain (WV) model [3].

Conventionally, the scaling of interface width (W) is used to determine the universality class of a discrete growth model. Usually, W, substrate size (L), and growth time (t) are related as $W(L,t) \sim L^{\alpha} f\left(\frac{t}{L^{z}}\right)$, which is called the Family-Vicsek scaling relation [4], when α is roughness exponent and z is dynamical exponent. The interface width is a function of time as $W(L,t) \sim t^{\beta}$, where β is growth exponent. In this method, three critical exponents (β, α, and z) are calculated and compared to the theoretical values of each universality class. When the growth exponent changes with the growth time, the system is said to have crossover.

In some growth models, it is difficult to obtain true asymptotic exponents because of finite size effects. Previous works [5-7] try to find more accurate critical exponents by determining the terms of the critical exponents. In our previous work, the expected asymptotic growth exponent of the DT model was found by using the correction-to-scaling technique. However, the asymptotic behavior of some models, such as the WV model, are still not clear.

Recently, a method involved roughness distribution in the steady state has been proposed [8-10] as an alternative technique to identify possible universality classes of the models. Reis Aarão and coworkers [11-14] have used the roughness distribution to study the ballistic deposition (BD), and the restricted solid-on-solid models and found that they are in the Kardar-Parisi-Zhang [15] (KPZ) scaling. This method has also been used [11-14, 16] to determine the universality class of models such as the collective diffusion, the limited mobility, the bidisperse ballistic deposition, and the grain deposition models.

In addition, Das Sarma and coworkers [17, 18] have suggested that using the multiple hit ($m>1$) and the long surface diffusion length ($\ell>1$) noise reduction techniques (NRTs) with the scaling of interface width can reduce stochastic noise until the asymptotic behavior of growth models are observed. They have also showed that the $m>1$ and the $\ell>1$ NRTs are equivalent in enhancing an asymptotic universality class of the DT model. The NRTs can be used to induce an unstable growth of the WV and Larger Curvature (LC) [19, 20] models in (2+1)- dimensional substrate systems.

In previous work [21], the roughness distribution with $m>1$ NRT has been used to find the universality class of the (1+1)-dimensional DT model. The results showed that the $m>1$ NRT may enhance the asymptotic roughness distribution of the (1+1)-dimensional DT model.

Consequently, determining asymptotic universality class of a discrete growth model with and without the NRTs by using the roughness distribution method is an interesting issue. Our aims are to use the roughness distribution method to identify the asymptotic universality class of thin film growth models and to study effects of NRTs on the roughness distributions of thin film growth models. We expect that universality

classes of various thin film growth models can be determined, and effects of the NRTs on roughness distributions of thin film growth models can be identified.

More realistic simulations are done on two-dimensional substrates which is denoted as (2+1) dimensional simulations. In this work, the roughness distribution of the (2+1)-dimensional BD [22], DT [1, 2], WV [3], LC [19, 20], and F [23] models are investigated. The NRTs, both the $m>1$ NRT and the $\ell>1$ NRT, are utilized. It is the first time that effects of the NRTs on the roughness distribution are investigated in the (2+1)-dimensional substrate systems. Additionally, the scaling of interface width of these noise reduced growth models at early times is also studied.

Moreover, in order to understand growth mechanisms in microscopic scale, it is necessary to characterize the grown surface morphologies. The height distribution may be used to characterize morphologies and to study the up-down symmetric property of thin films. So, we also study the height distributions of growth models that provide important growth modes: layer-by-layer growth mode and mound formation.

A layer-by-layer growth is a characteristic of high quality surface growth. A well-known technological process used to produce high quality thin films is Molecular Beam Epitaxy (MBE) [24]. A high temperature MBE growth enables one to produce smooth thin films, since a high substrate temperature yields higher surface diffusion that gives rise to the layer-by-layer growth. In growth simulation, this event is identified by oscillations of interface width. The $m>1$ NRT [18, 25, 26] and the $\ell>1$NRT [18, 26] are used to enhance the layer-by-layer growth.

In studies of mound formation, the NRTs can be used to produce mounded morphology [26, 27] in the (2+1)-dimensional LC and WV models. Mound formation is discussed in thin film growth both in simulations and in experiments [27-30]. Our purpose is to consider the height distribution of the mounded morphologies and to study effects of substrate size on the height distribution of the mounded surfaces.

Overview of the dissertation

In this dissertation, thin films are simulated using the BD, DT, WV, LC, and F models with and without the $m>1$ NRT and the $\ell>1$ NRT on (2+1)-dimensional substrate systems. This thesis is organized as following. Chapter I is the introduction: the background, the motivation, and the objectives. Modeling and theories regarding

the BD, DT, WV, LC, and F models, the continuum growth equations, along with details of the NRTs and quantities of interest are explained in chapter II. In chapter III, surface morphologies and scaling of interface width of the growth models with and without the NRTs, are shown and discussed. The effects of the NRTs on the growth exponent are also presented in this chapter. In chapter IV, we show roughness distributions of the growth models with and without the NRTs, and also present finite size effects on the roughness distribution of growth models. In Chapter V, the height distribution of the growth models with and without the NRTs are shown and finite size effects on the height distribution of growth models are presented. Finally, we conclude our study in chapter VI.

CHAPTER II

MODEL AND THEORY

In this chapter, we discuss growth models with and without the NRTs. Moreover, continuum growth equations used to describe the possible universality classes of the models will be presented. Important quantities such as interface width, roughness distribution, and height distribution will be defined. Scaling relation will be explained.

2.1 Growth models and universality class

In our work, various thin film growth models: the BD, DT, WV, LC, and F models were simulated in (2+1)-dimensional substrate systems with and without the NRTs. Nowadays, the asymptotic behavior of the BD, LC, and F models are well known, whereas asymptotic universality class of the DT and WV models are difficult to observe in simulation study.

2.1.1 The BD, DT, WV, LC, and F models

The BD [22] model is a discrete porous aggregation model, whereas the DT [1, 2], WV [3], LC [19, 20], and F [23] models are discrete solid-on-solid (SOS) models proposed in the early 1990s for the study of kinetic surface roughening in thin film growth. The SOS conditions mean that desorption, overhanging, and vacancy are not allowed. These conditions correspond to the ideal MBE growth. In all models, an atom is deposited on a substrate on a randomly chosen site. After arriving at the surface, the newly deposited atom can move according to surface diffusion rules of each model as illustrated in Fig. 2.1.

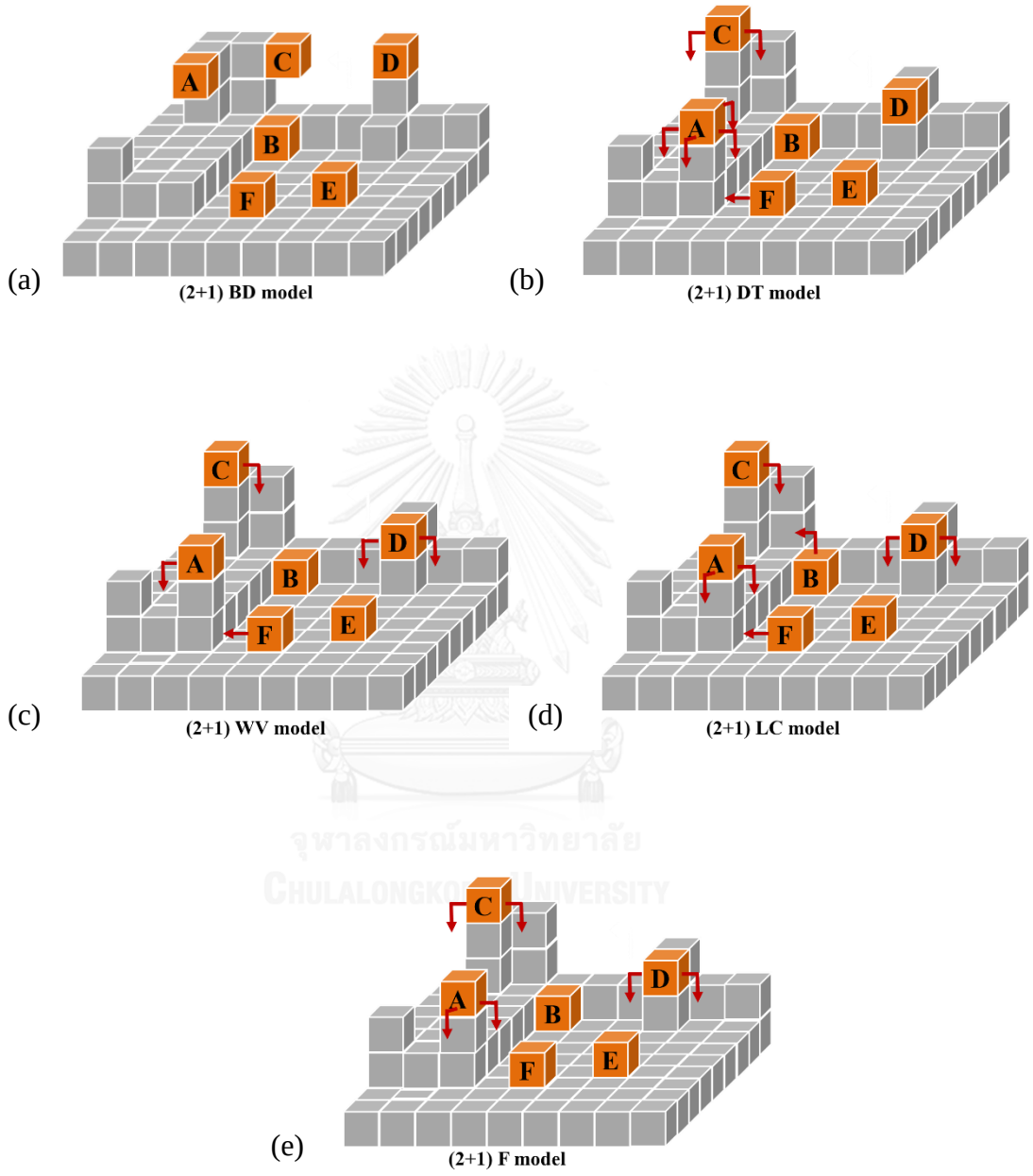

Fig. 2. 1 Diagrams illustrating diffusion rules of the (2+1)-dimensional (a) BD, (b) DT, (c) WV, (d) LC, and (c) F models. The adatom moves in the direction indicated by the arrows.

In the BD model (Fig. 2.1(a)), the atom is deposited at a randomly chosen site. It is incorporated at the first site that it comes into contact with the film. Bond formation at the first contact makes it possible to have void defects in the grown films (atoms A and C). The BD model is selected for studying in this work because this model is well-known as a porous aggregation model.

In the DT model (Fig. 2.1(b)), only an atom without a lateral bond can move to one of its nearest neighbors where it can form at least one lateral bond. If only one of the nearest neighbors provides the lateral bond, the atom moves directly to that site (atoms F). If more than one nearest neighbors meet this condition, one of them is chosen by random (atoms A and C follow one of the arrows with equal probability). However, if none of the nearest neighbor can provide a lateral bond, the atom stays at its deposition site (atom E). An atom that is deposited at a site with at least one lateral bond also remains at its deposition site (atoms B and D). The DT model is chosen to investigate its roughness distribution because it is difficult to see the true asymptotic behavior of this model. The DT model can be used to study the thin film growth at low temperature.

In the WV model (Fig. 2.1(c)), an atom moves to find the site with the maximum number of bonds. There are two differences in the WV and DT diffusion rules. Firstly, an atom that already has one lateral bond can move to a site that can provide more bonding in the WV model but is not allowed to move in the DT model. This is illustrated by atom D which does not move in the DT model (Fig. 2.1(b)) but moves to its nearest neighbor which provides more bonds in the WV model (Fig. 2.1(c)). Secondly, a diffusing atom only moves to a site with at least one lateral bond in the DT model, while it seeks the site with the maximum number of bonding in the WV model. This point is seen clearly in atom C which can moves to either left (one lateral bonds) or right (two lateral bond) in the DT model (Fig. 2.1 (b)) but will only move to its right in the WV model (Fig. 2.1 (c)). We study the WV model because the scaling of interface width cannot be used to find asymptotic universality of this model [2]. Additionally, the WV model can be used to study the mound formation of thin film growth.

In the LC model, an atom moves to a nearest neighbor that provides the largest curvature. The curvature at each site can be calculated from

$\nabla^2 h = h(x+1) + h(x-1) - 2h(x)$ for the (1+1)-dimensional growth and

$\nabla^2 h = h(x+1, y) + h(x-1, y) + h(x, y+1) + h(x, y-1) - 4h(x, y)$ for the (2+1)-dimensional growth when $h(x, y)$ is the height of the deposition site (x, y) on the substrate. Fig. 2.1(d) shows how adatoms move in the (2+1) LC model. Atom C moves to the right and atoms B and F move to the left because they have the largest curvature among the nearest neighbors. If the curvature of the deposited site and its neighbors are equal, the atom does not move (atom E). Finally, if the curvature of the neighboring sites are the same, but larger than that of the deposition site, one of the neighbors is chosen randomly (atoms A and D). The LC model can be used to study the mound formation of thin film growth. Its asymptotic behavior should belong to the linear fourth-order equation by construction.

According to the F model (Fig. 2.1(e)), after atom arrives on the surface, it can move to its nearest neighbors that provide the smallest height. If the height of the neighbors are the same as at the deposition site, the atom does not move (atom B, E, and F). If the height of the neighboring sites and the deposition site are the same, one of the neighbors is chosen randomly (atoms A, C, and D). The F model is used to study the growth that depends on the gravitational force instead of the bond formation.

2.1.2 Universality class of the Growth models

The scaling functions and critical exponents are used to define the universality class of growth models [22, 31]. Two growth models that have the same critical exponents and scaling function belong in the same universality class [22, 31]. Continuum growth equations are used to study behavior of the interface in large length scale. The critical exponents investigated from a discrete growth model should be consistent with the corresponding continuum growth equation describing that model [22].

The BD model belongs to the KPZ scaling which can be described by a continuum equation:

$$\frac{\partial h(x,t)}{\partial t} = \nu_2 \nabla^2 h + \lambda_2 (\nabla h)^2 + \eta \qquad (2.1)$$

where ν_2, and λ_2 are growth coefficients, h is the surface height at position x and time t, and η is the Gaussian noise associated with the incident beam fluctuation. The $\nu_2\nabla^2 h$ term leads to a smoothing effect of the surface for a positive ν_2 while a negative ν_2 leads to unstable growth with mounded morphologies. The nonlinear term $\lambda_2(\nabla h)^2$ yields a bump on the interface called the lateral growth. The film grown with this nonlinear term has larger local slope in the interface and the average height of the surface is increased [22].

Identifying universality class of the (2+1)-dimensional DT model is quite complicated due to many crossovers [7]. Das Sarma and coworkers [17] use the $m>1$ NRT and suggest that the (2+1) DT model can be described by a continuum growth equation:

$$\frac{\partial h(x,t)}{\partial t} = \nu_2\nabla^2 h - \nu_4\nabla^4 h + \sum_{n=1,2,3,\ldots} \lambda_{2(2n)}\nabla^2(\nabla h)^{2n} + \eta \qquad (2.2)$$

where ν_2, ν_4 and $\lambda_{2(2n)}$ are growth coefficients. They found that [17] ν_2 is extremely small but not negligible. The $-\nu_4\nabla^4 h$ term describes the relaxation due to surface diffusion. From equation (2.2), the asymptotic universality class of the (2+1) DT model should be the Edwards-Wilkinson (EW) universality class. The continuum growth equation that describes the EW universality class is [22]

$$\frac{\partial h(x,t)}{\partial t} = \nu_2\nabla^2 h + \eta \qquad (2.3)$$

where ν_2 is a surface tension. The critical exponents of the EW universality class can be written in the following forms [22]: the growth exponent $\beta = (2-d)/4$, the roughness exponent $\alpha = (2-d)/2$, and the dynamical exponent $z = 2$ when d is the dimension of the substrate. Chame and Aarão Reis [32] studied the evolution of effective dynamical exponent (z) which confirmed that the (2+1) DT model belonged asymptotically to the EW universality class. In this work, we investigate the universality class of both the original and the noise reduced DT models in (2+1)-dimensions by studying the roughness distribution [6, 8, 9, 11, 13, 16].

Identifying asymptotic behavior of the (2+1) dimensional WV model is not straight forward either. It has been reported that values of the critical exponents in the (2+1)-dimensional WV model are $\beta = 0.20 \pm 0.20$ and $\alpha = 0.66 \pm 0.03$ [22], while Das Sarma and Ghaisas [33] found that $\beta = 0.192 \pm 0.002$. These are close to the values from the Villain-Lai-Das Sarma (VLDS) equation [34];

$$\frac{\partial h(x,t)}{\partial t} = -\nu_4 \nabla^4 h + \lambda_{22} \nabla^2 (\nabla h)^2 + \eta(x,t) \tag{2.4}$$

which can be approximated by [22] $\beta = (4-d)/(8+d)$, $\alpha = (4-d)/3$, and $z = (8+d)/3$. Note that these expressions are not exact. There was a detailed numerical study [4] and a theoretical work using renormalized field theory [23] to explain the origin of higher order corrections to these values. Later, Krug [35] and Siegert [36] studied the global particle diffusion current in the (100) direction of the original WV model and found the current to be downhill which indicates that the asymptotic universality class of the (2+1) dimensional WV model should be the EW universality class. However, Das Sarma and coworkers [17, 26, 28] found uphill current in the (111) direction of both the original and the noise reduced WV model. The uphill current is temporary before crossing over to downhill current in the original WV model while the $m > 1$ WV model yields very strong uphill current. This information suggests that the (2+1) dimensional WV model is unstable with mounded morphology. This result has been confirmed by Ref. [27]. Recently, Chame and Aarão Reis [32] used the scaling of the local interface width of the (2+1) dimensional WV model and showed that the effective dynamical exponent converged to $z \approx 2$ (when $t \to \infty$) which is consistent with the value of z in the EW universality class. From previous works [17, 26, 28, 32, 33, 35-37], it is clear that scaling behavior of the WV model is far from trivial. In our work, we attempt to study the (2+1)-dimensional WV model using the roughness distribution of the NRT growth simulations.

By construction, the LC model should be in the Kim-Das Sarma class [19] described by the linear fourth-order equation (the Mullins-Herring, MH):

$$\frac{\partial h}{\partial t} = -\nu_4 \nabla^4 h + \eta \,. \tag{2.5}$$

According to its diffusion rules, the F model is in the linear second-order scaling or EW class [22] defined by Eq. (2.3). The LC and F models are chosen for our study for the sake of comparison. The model is linear and obtaining its universality class should be quite straightforward.

2.2 The Growth models with the NRTs

The NRT has been used [17, 18, 26] to study the universality class of discrete growth models via calculation of the critical exponents. Two different techniques have been used in the literature: the $m>1$ [17, 18, 25, 26, 38] and the $\ell>1$ [17, 18, 26, 38] NRTs. In general, $m>1$ NRT and $\ell>1$ NRT can induce layer-by-layer-growth in early time [18, 25, 38], and lead to asymptotic behavior at later time [17, 18]. Additionally, the $m>1$ NRT has previously been used [21] in the study of the roughness distribution of (1+1)-dimensional DT model. The result has been shown that the $m>1$ NRT may lead to the asymptotic universality class of the (1+1)-dimensional DT model.

2.2.1 Multiple hit noise reduction technique

In growth simulations, the $m>1$ NRT is a well-known technique used to reduce the stochastic noise due to the incident beam fluctuation. It is only a computational technique without any real physical meaning. A multiple hit parameter m is the number of time a site must be selected before an actual incorporation can occur. Each site has its own counter. When a site is selected, the counter of that site is increased by one but the height of that site remains the same until the counter reaches the multiple hit parameter (m), which is an integer (m = 1 for the original model), then the height of that site is increased by one and the counter is reset to zero. Fig. 2.2 shows an example for the $m>1$ NRT when m equals 3. Starting with a flat substrate with both height and counter at all sites are zero, if site number 5 is selected, the counter of the site, C_5, is increased by 1 ($C_5 = 1$) and the height is still equal to 0 ($h_5 = 0$). Next round, site number 2 is chosen, the counter C_2 is increased by one ($C_2 = 1$) and its height is zero ($h_2 = 0$). In third round, if site number 5 is chosen again, its counter is increased to $C_5 = 2$ and its height is still equal to zero. For the fourth round, if site number 5 is selected again, so

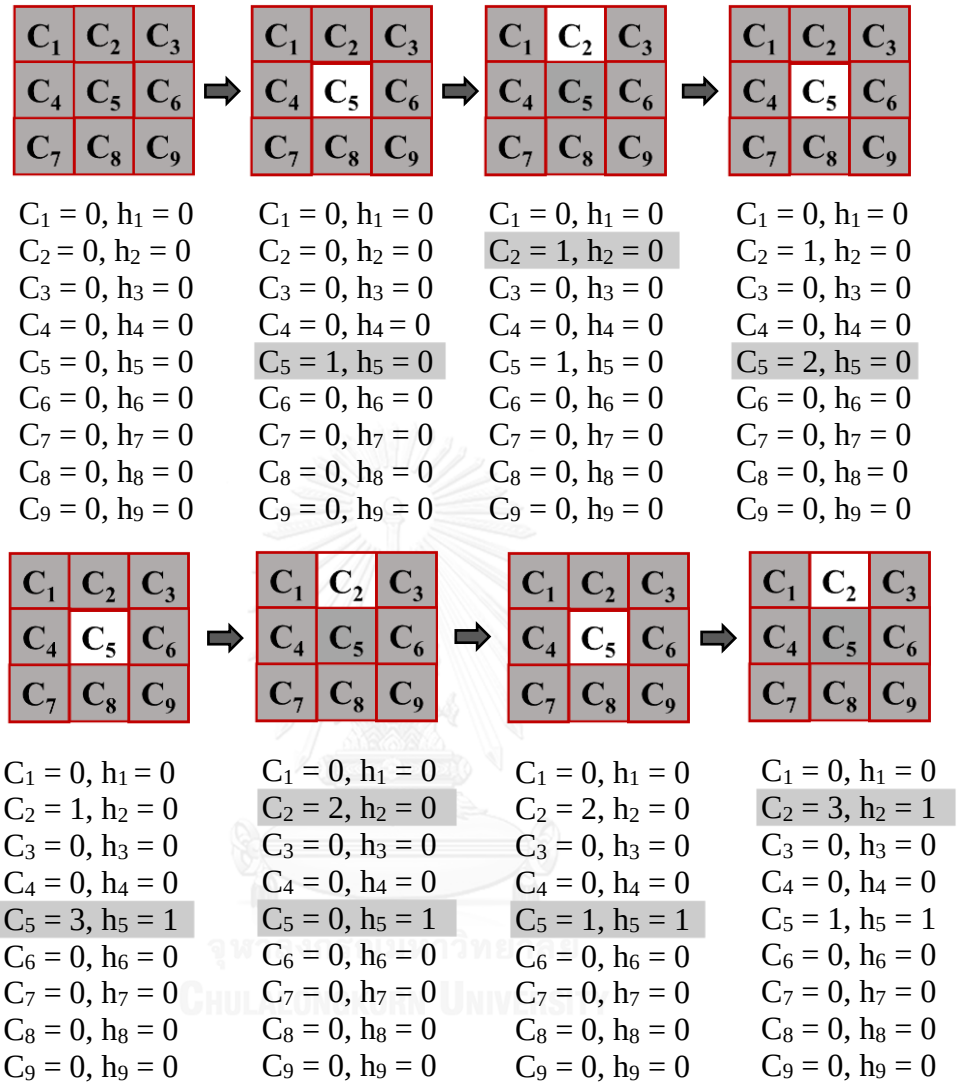

Fig. 2. 2 Illustrations of the $m > 1$ NRT in the case that m = 3 on (2+1)-dimensional flat substrates. After deposited atom selects its final site, the counter of that site is increased by one but its height does not change until the counter is equal to 3.

$C_5 = 3$. Since $C_5 = m$, the height is increased by one and $h_5 = 1$, the counter C_5 is then reset to zero ($C_5 = 0$).

2.2.2 Long surface diffusion length noise reduction technique

The $\ell > 1$ NRT has also been used as a noise reduction technique [17, 18, 26, 38]. This is a technique that increases the lateral length that each atom can move. This can be done by increasing the number of time an atom is allowed to hop. In our work, we have defined the parameter ℓ as a maximum number of times that the diffusing atom can hop to find the final site under diffusion rules of the original models.

In the DT model with the $\ell > 1$ NRT, an atom without a lateral bond is allowed to hop in order to increase its number of bond just as in the original model. However, it can hop more than once. The hopping stops when the number of hop is ℓ or the number of lateral bond is at least one. Let us consider atom E in Fig. 2.1(b) which stays at its deposition site in the original model. But if, for example, $\ell = 3$, diffusion process for atom E will be as following. For the first round, it checks its nearest neighbors, neither can provide any lateral bond so one is chosen by random. If the neighbor on its left is chosen, atom E moves to one left. In the second round, it checks its neighbors again and finds that the neighbor does not provide a lateral bond, so atom E moves to the neighbor by a random again. If the neighbor on its left is chosen, in third round, atom E will be grown on the film with one lateral bond. Note that this variation of the DT model is practically the same as the limited mobility model studied in Ref. [11].

In the original WV model, a deposited atom diffuses to find the site with the maximum number of bond, which is five in the 2-dimensional substrate systems. When the $\ell > 1$NRT is implemented, each newly deposited atom repeats the diffusion process ℓ times. In each step, the atom compares number of bond it can form at its present site and at its nearest neighbor sites. If at least one nearest neighbor can offer more bonding than the present site, the atom hops to the neighbor with the maximum bonds. If the maximum number of bond the nearest neighbors can provide is the same as at the present site, the atom chooses among the neighbors with the maximum bonds and the present site with equal probability. However, if all nearest neighbors provide less bonds than the present site, the atom remains at the present site and the diffusion process ends here even when the number of hop is still less than ℓ.

In the LC model, an atom moves to one of its nearest neighbors that provide the largest curvature. The $\ell > 1$ NRT is applied in the same way as the WV model described above. Note that an atom can move to its nearest neighbors that provide larger or the same curvature compared to the initial site. The hopping will stop when the atom finds a site that has the largest curvature or the number of hop is ℓ.

For the F model with the $\ell > 1$ NRT, an atom can move to its nearest neighbors that provide smaller or equal height compared to the initial site. The hopping will stop when the atom finds a site that has the lowest height or the number of hop is ℓ, whichever comes first.

Note also that the growth models studied here are valid only for a certain range of temperature which is high enough for surface atoms to diffuse but not enough for them to desorb. This mean the value of ℓ cannot be too large.

2.3 Quantities of interest

Quantities used in this work are interface width (W), roughness distribution, and the height distribution. Qualitative characterization of the distributions such as skewness (S), and kurtosis (Q) are also studied.

2.3.1 Interface width

The first quantity of interest is the interface width which is the standard deviation of the surface height and is defined, for 2 dimensional substrate systems with a substrate of $L \times L$ lattice sites, as

$$W(L,t) = \left\langle \left[\frac{1}{L^2} \sum_{x=1}^{L} \sum_{y=1}^{L} \left[h(x,y,t) - \bar{h}(t) \right]^2 \right]^{1/2} \right\rangle . \tag{2.6}$$

Here, $h(x,y,\mathrm{t})$ is the height of site (x,y) at time t, $\bar{h}(t)$ is the average height of the surface at time t and the bracket, $\langle\ \rangle$, denotes a configurational average. In this work, 50-100 configurations were used. The plot of interface width versus time consists of two regions separated by a crossover time or saturation time (t_{sat}). At early time ($t << t_{sat}$), the interface width increases as a power of time

$$W(L,t) \sim t^{\beta}, \tag{2.7}$$

where β is the growth exponent. At large time, ($t >> t_{sat}$), the interface width reaches a saturated value (W_{sat}) that depends on the substrate size:

$$W_{sat}(L) \sim L^{\alpha}, \tag{2.8}$$

where α is the roughness exponent. Furthermore, the saturation time also depends on the substrate size,

$$t_{sat} \sim L^{Z}, \tag{2.9}$$

where z is the dynamical exponent. These three critical exponents obey scaling relation,

$$z = \frac{\alpha}{\beta}. \tag{2.10}$$

Interface width is plotted as a function of time in monolayers (MLs) on a log-log scale. A monolayer means that the number of deposited particles during that time divide by number of lattice sites on the substrate; $L \times L$. Slope of the best linear fit is the growth exponent β. In the saturation regime or the steady state, the interface width becomes steady. This constant width, W_{sat}, depends on the system size. If we plot W_{sat} versus L on a log-log scale. The data should be a straight line with the slope being the roughness exponent α.

2.3.2 Roughness distribution

The second quantity calculated in this work is the probability density of squared width, $P(W^2)$, also known as the roughness distribution [8-10]. Previous works [8-10, 21] have shown that growth models belonging to the same universality class have the same roughness distribution. During simulations, the squared interface width is calculated in different configurations, i.e. growth at different time instants, within the saturation regime. $P(W^2)$ is the probability that the squared width of a given configuration lies within the range $\left[W^2, W^2 + dW^2\right]$. Over 10^8 configurations are used for each roughness distribution in our work.

The roughness distributions obey a scaling relation of the form [10, 14, 16, 21]

$$P\left(W^2\right)=\frac{1}{\sigma}\Psi\left(\frac{W^2-\left\langle W^2\right\rangle}{\sigma}\right). \tag{2.11}$$

Here Ψ is the universal function [6, 10, 16, 21], σ is the standard deviation calculated from

$$\sigma=\sqrt{\left\langle\left(W^2\right)^2\right\rangle-\left\langle W^2\right\rangle^2}, \tag{2.12}$$

and the average of squared width is

$$\left\langle W^2\right\rangle=\frac{\sum_{i=1}^{N}W_i^2\ P\left(W_i^2\ \right)}{\sum_{i=1}^{N}P\left(W_i^2\ \right)} \tag{2.13}$$

when N is the number of configurations. The roughness distribution can be quantitatively analyzed with skewness $\left(S\right)$ and kurtosis (Q) [39] which are

$$S=\left\langle\frac{1}{N}\sum_{i}^{N}\left(W_i^2-\left\langle W_i^2\right\rangle\right)^3\Bigg/\left(\frac{1}{N}\sum_{i}^{N}\left(W_i^2-\left\langle W_i^2\right\rangle\right)^2\right)^{\frac{3}{2}}\right\rangle\text{, and} \tag{2.14}$$

$$Q=\left\langle\left(\frac{1}{N}\sum_{i}^{N}\left(W_i^2-\left\langle W_i^2\right\rangle\right)^4\Bigg/\left(\frac{1}{N}\sum_{i}^{N}\left(W_i^2-\left\langle W_i^2\right\rangle\right)^2\right)^2\right)-3\right\rangle. \tag{2.15}$$

If $S=0$, the height distribution is a normal distribution (Fig. 2.3(a)); if $S>0$, it is called positively skewed and the height distribution has a longer right tail (Fig. 2.3(b); and if $S<0$, it is called negatively skewed and the height distribution has a longer left tail (Fig. 2.3(c)). In analyzing film morphology, $S=0$ indicates an up-down symmetry. As for the kurtosis, $Q=0$ indicates a normal distribution (Fig. 2.4(a)) while positive and negative Q shows a peaked distribution (Fig. 2.4(b)) and a flat distribution (Fig. 2.4(c)) relative to a normal distribution respectively.

2.3.3 Height distribution

In this work, we also study the height distribution, $P_h\left(\Delta h\right)$, which is the probability density of the height relative to the average height ($\Delta h=h-\bar{h}$). $P_h\left(\Delta h\right)$ is the

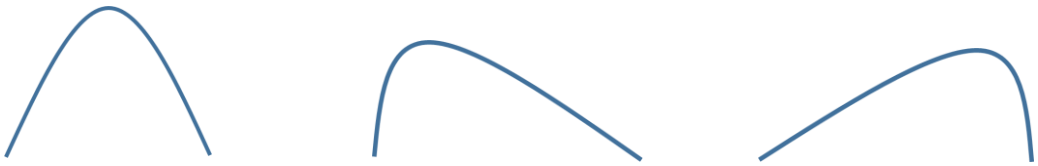

Fig. 2. 3 Illustrations geometrical characteristics of the distribution according to the value of S

Fig. 2. 4 Illustrations geometrical characteristics of the distribution according to the value of Q

probability that Δh of a given configuration lies within the range $[\Delta h, \Delta h + dh]$. In previous work [12], the scaling of height distribution is $P_h(\Delta h) = \frac{1}{\sigma_h} P_h(\Delta h / \sigma_h)$ when σ_h is the root mean square fluctuation of Δh. It was used to discuss the height distributions of growth models in the KPZ [15] scaling. Quantitative characterization of the height distribution can be done by studying the skewness (S) and the kurtosis (Q) which can be written as [12]

$$S = \left\langle \frac{1}{L^d}\sum_i^{L^d}(\Delta h)^3 \Big/ \left(\frac{1}{L^d}\sum_i^{L^d}(\Delta h)^2\right)^{\frac{3}{2}} \right\rangle \tag{2.16}$$

$$Q = \left\langle \left(\frac{1}{L^d}\sum_i^{L^d}(\Delta h)^4 \Big/ \left(\frac{1}{L^d}\sum_i^{L^d}(\Delta h)^2\right)^2 \right) - 3 \right\rangle \tag{2.17}$$

where L is the substrate size and d is the dimension of the substrate. The < > represent the ensemble average.

In analyzing surface morphology, $S = 0$ indicates an up-down symmetry. As for the kurtosis, $Q = 0$ indicates a normal distribution while positive and negative Q means a peaked distribution and a flat distribution relative to a normal distribution respectively.

CHAPTER III

RESULTS AND DISCUSSIONS: SURFACE MORPHOLOGY AND INTERFACE WIDTH OF GROWTH MODELS

In this chapter, surface morphology, interface width, and growth exponent of the BD, DT, WV, and LC models with and without the NRTs will be presented. Firstly, time evolution of surface morphologies and interface width with and without the NRTs will be presented. Secondly, effects of the NRTs parameters on the growth exponent of the growth models will be discussed.

Thin film growth with the BD, DT, WV, and LC models in (2+1)-dimensional substrate systems were simulated. Substrates of size $L \times L$ lattice sites are used. The value of L used in this chapter is $L = 100$. The size $L = 100$ is large enough to show the behavior of each model because the finite size effects on the roughness distributions of the DT, WV, and LC models are not strong. All models were simulated up to the steady state (more than 10^6 MLs for the BD, DT, and WV models, and more than 10^7 MLs for the LC model). Effects of the NRTs on the surface morphologies and interface width are investigated. The interface width is averaged over 50 to100 configurations.

3.1 Surface morphologies of growth models with and without the NRTs

In this section, all morphologies are plotted on the same scale for easy comparison. The variable on the height axis is, in fact, the height fluctuation, $h - \bar{h}$. Each figure shows a section of 100×100 lattice sites from a morphology at time t.

Morphologies and an effects of the NRTs on surface morphologies of the BD, DT, WV, and LC models are shown.

Firstly, we present the surface morphologies of the BD model with and without only the $m>1$ NRT. The $\ell>1$ NRT cannot be used to reduce the noise for the BD model because the long surface diffusion length technique cannot be incorporated to the BD diffusion rule. Fig 3.1 shows surface morphologies for original BD model ($m=1$) at t = 0.5 MLs, 3.3×10^{3} MLs, 3.3×10^{6} MLs. In the noise reduced BD model, when m is increased, for example; $m=1$, 3, 5, and 25 as shown in Fig. 3.2, surface morphologies become smoother as m increased . This means that a void defect of the film grown with the noise reduced BD model is smaller than the original BD model. So, the $m>1$ NRT can reduce a void defect of film grown by a porous aggregation model.

In the DT model, the effects of both the NRTs on morphologies are investigated. The morphologies grown with the DT model are shown in Fig. 3.3. The surfaces here are in a saturation region. Fig.3.3 (a) shows the surface of the original DT model that we can see a lot of high surface steps and deep grooves. When the noise is reduced with $m=3$, the surface in Fig. 3.3(b) is much smoother than in Fig. 3.3 (a), with further noise reduction at $m=5$ in Fig. 3.3 (c), the high steps and deep grooves become smaller as *m* increased. Similarly, the surface from the DT model with $\ell>1$ NRTs become smoother as ℓ increased. In Fig. 3.3(d) is morphology that the noise is reduced with $\ell=25$. The long surface diffusion length induces reducing the deep grooves by increasing probability of atom diffusion to search for the grooves and be incorporated there. So, the morphologies become smoother with increasing ℓ. Comparing the NRTs, we see that both of them are equivalent to produce smoother surface for the film grown by the DT model. These agree with previous works [17, 25, 38].

For the WV model, the surfaces from the original WV model shown in Figs. 3.4 (a) – 3.4(b) suggest that the surface becomes rougher with increasing deposition time. In order to investigate the effects of the $m>1$NRT, the surface of the WV with the noise reduced $m=5$ is presented in Fig. 3.5. At early time (1.0 ML) in Fig 3.5 (a), the morphology is smoother than the original model in Fig 3.4 (a) because the noise reduction yields the layer-by-layer growth [17]. Later, at 1.0×10^{3} MLs in Fig 3.5 (b),

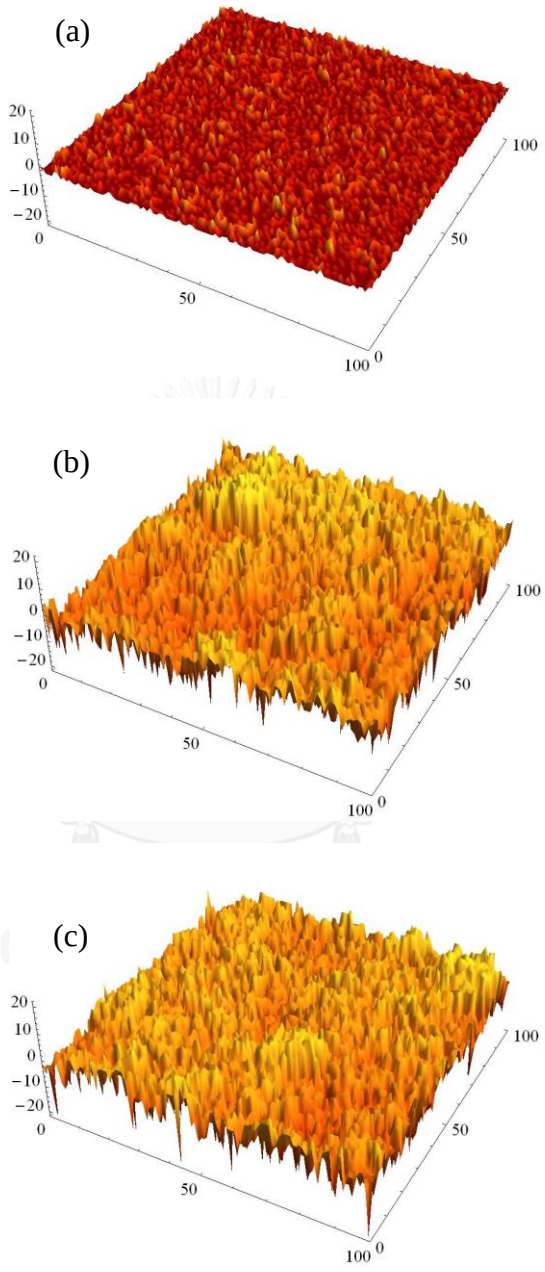

Fig. 3. 1 Surface morphologies of the BD model with m = 1 and at t (a) 0.5 MLs (b) 3.3×10^{3} MLs, and (c) 3.3×10^{6} MLs

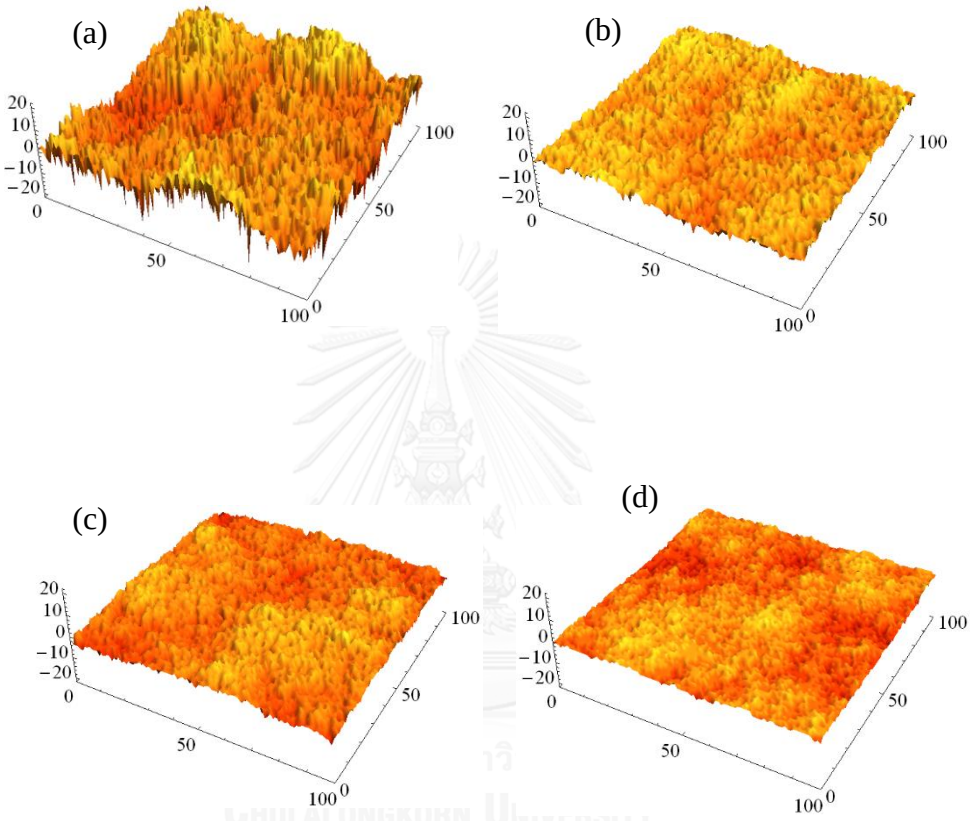

Fig. 3. 2 Surface morphologies of the BD model when (a) $m=1$ (original model) (b) $m=3$, (c) $m=5$, and (d) $m=25$ at the same time in the steady state.

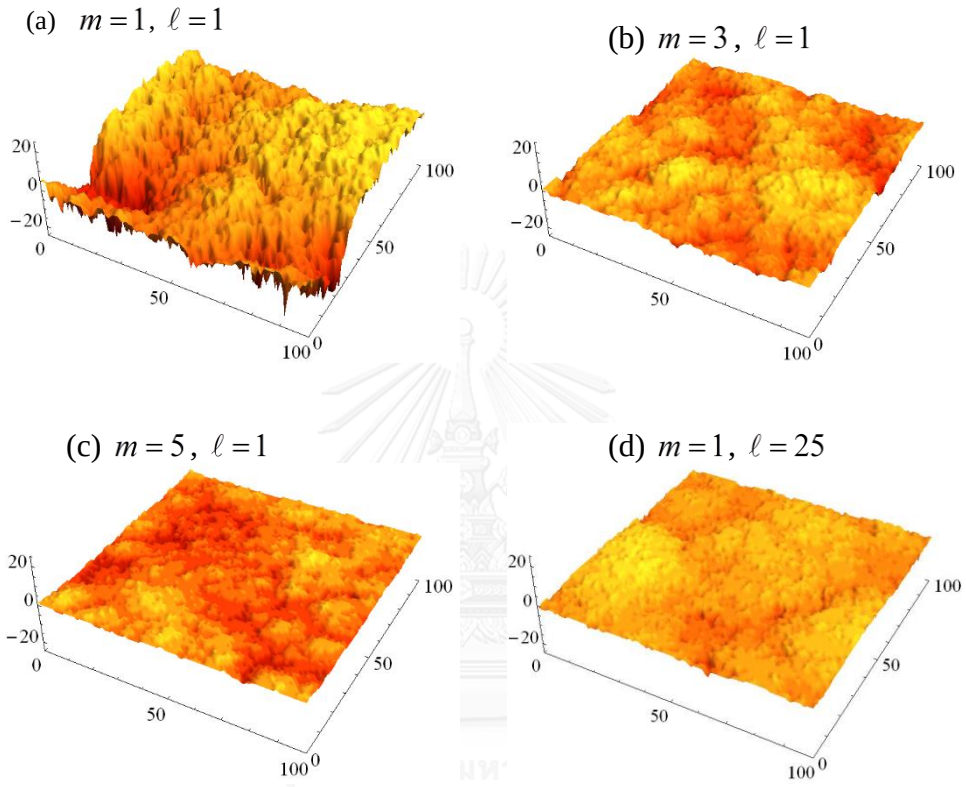

Fig. 3. 3 Surface morphologies of the DT model when (a) $m=1$ and $\ell=1$, (b) $m=3$ and $\ell=1$, (c) $m=5$ and $\ell=1$, and (d) $m=1$ and $\ell=25$ at the same time in the steady state.

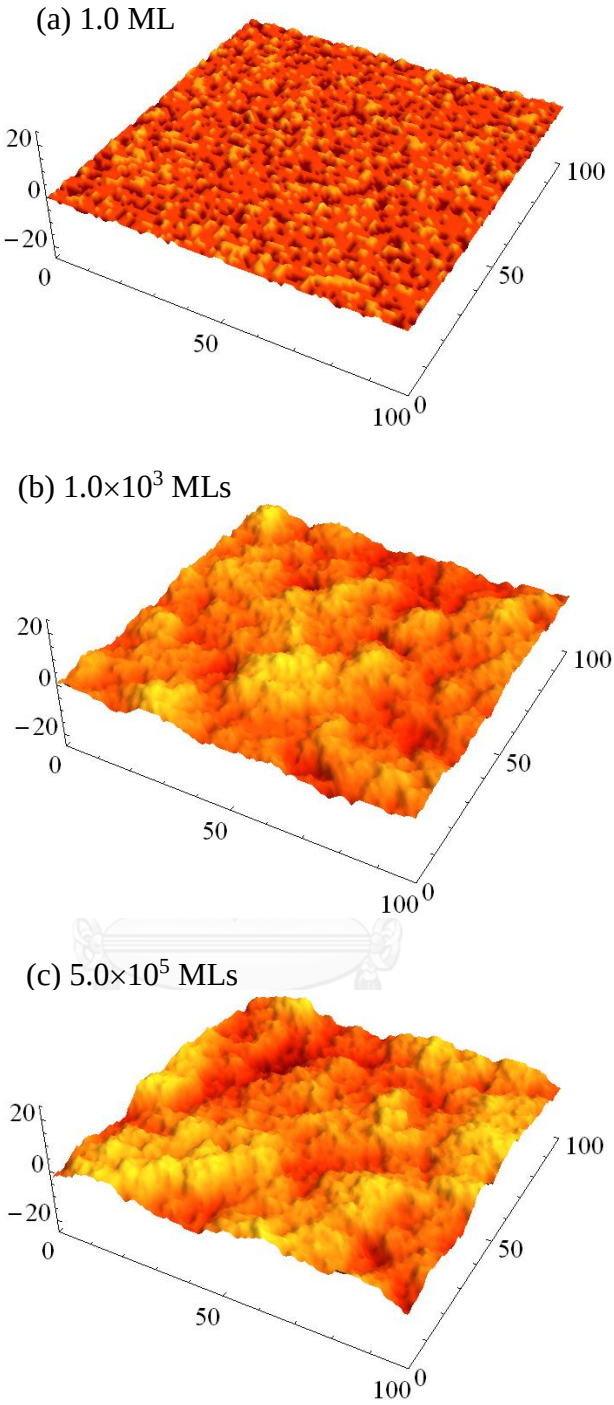

Fig. 3. 4 Surface morphologies of the WV model with m = 1, $\ell = 1$ at t (a) 1.0 MLs (b) 1.0×10^3 MLs, and (c) 5.0×10^5 MLs

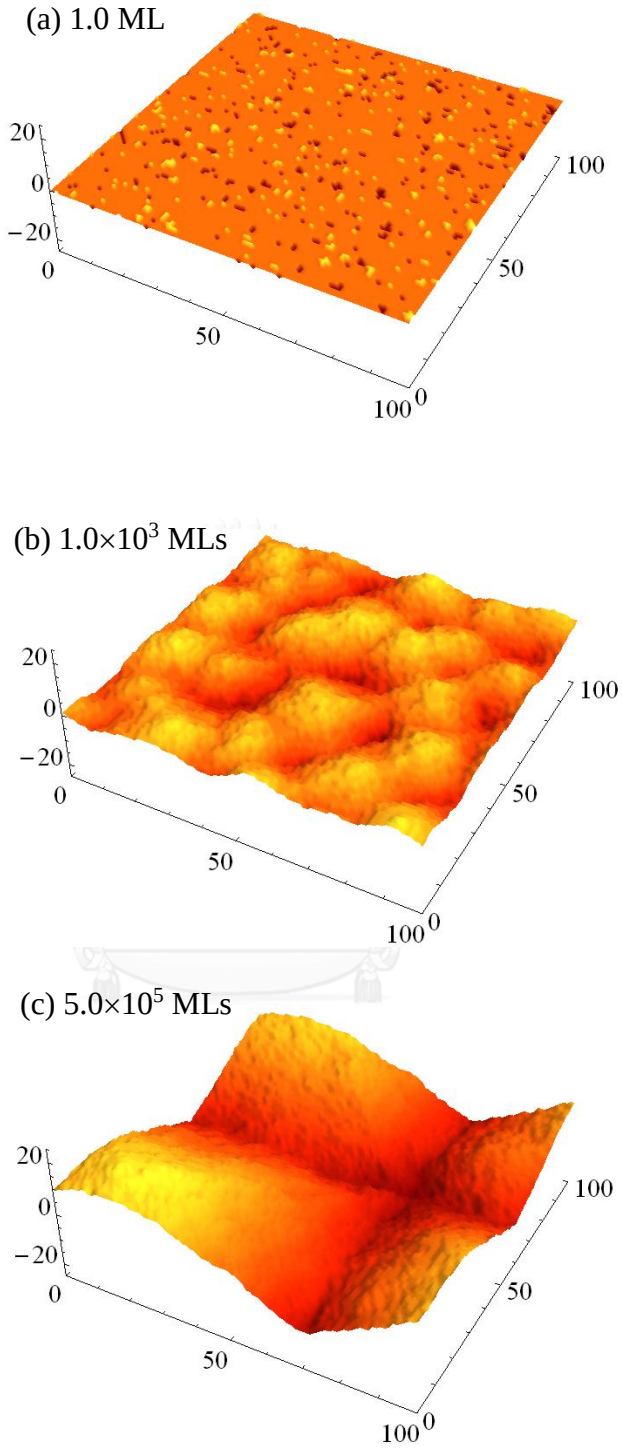

Fig. 3. 5 Surface morphologies of the WV model with the $m = 5$ and $\ell = 1$ at t (a) 1.0 MLs (b) 1.0×10^{3} MLs, and (c) 5.0×10^{5} MLs

specular mounding pattern caused by a non-equilibrium edge diffusion effect [28] can be seen, which is step edge diffusion (SED) instability [26]. This also shows that the $m>1$ NRT enhances a local uphill particle current [26]. At the steady state, at 5.0×10^5 MLs in Fig 3.5(c), mound formation becomes a single mound, in agreement with previous works [26-28].

In the WV model with the $\ell>1$ NRT, the noise is reduced with $\ell=25$ illustrated in Fig. 3.6 suggests that increasing ℓ induces the smooth surface at early time in Fig. 3.6(a), leads a specific mounding pattern in Fig. 3.6(b), and yields a single mounded morphology at the steady sate in Fig. 3.6(c). So, the ℓ>1 NRT can enhance the layer-by-layer growth and the mounded morphology same as the $m>1$ NRT. Our results help complete the study of the mounding instability in epitaxial growth model, which have been deeply discussed in Ref. [26] and [28]. Additionally, we found that the mounded surface can be clearly seen when $m>3$ for the $m>1$ NRT and $\ell\geq5$ for the $\ell>1$NRT.

For the LC model morphology, time varying surface grown with the original LC model is presented in Fig. 3.7(a) - 3.7(c). The film roughness is increased with increasing deposition time. When the NRTs are incorporated into the LC model, we found that both the $m>1$ and the $\ell>1$ NRTs induce the mounded growth in the LC model shown in Fig. 3.8 and Fig. 3.9. In Fig. 3.8(a) and Fig. 3.9(a), the small islands appeared, however, the surface in Fig. 3.8(a) seems smoother than the surface in Fig. 3.9(a) this is because the $m>1$ NRT leads to layer-by-layer-growth in the LC model, whereas the $\ell>1$ NRT cannot induce the smooth surface, unlike the $m>1$ NRT. the $\ell>1$ NRT immediately yields the mounding at early time. In Fig 3.8(b) and 3.9(b), the surfaces are in the kinetically rough growth region at 1.0×10^3 MLs. When the noise is reduced with parameter $m=5$ in Fig 3.8(b), the mounded surface clearly appear. Similarly, when ℓ is increased, for example; $\ell=25$ in Fig 3.9(b), the specific mounded morphology is emerged. At the steady state (1.0×10^6 MLs), a single mounded morphology is clearly seen as shown in Fig 3.8(c) for the noise is reduced with the $m>1$ NRT and in Fig 3.9 (c) for the noise is reduced with the $\ell>1$ NRT. In our work, we found that the mound formation is exhibited when $m>3$ for the $m>1$ NRT and

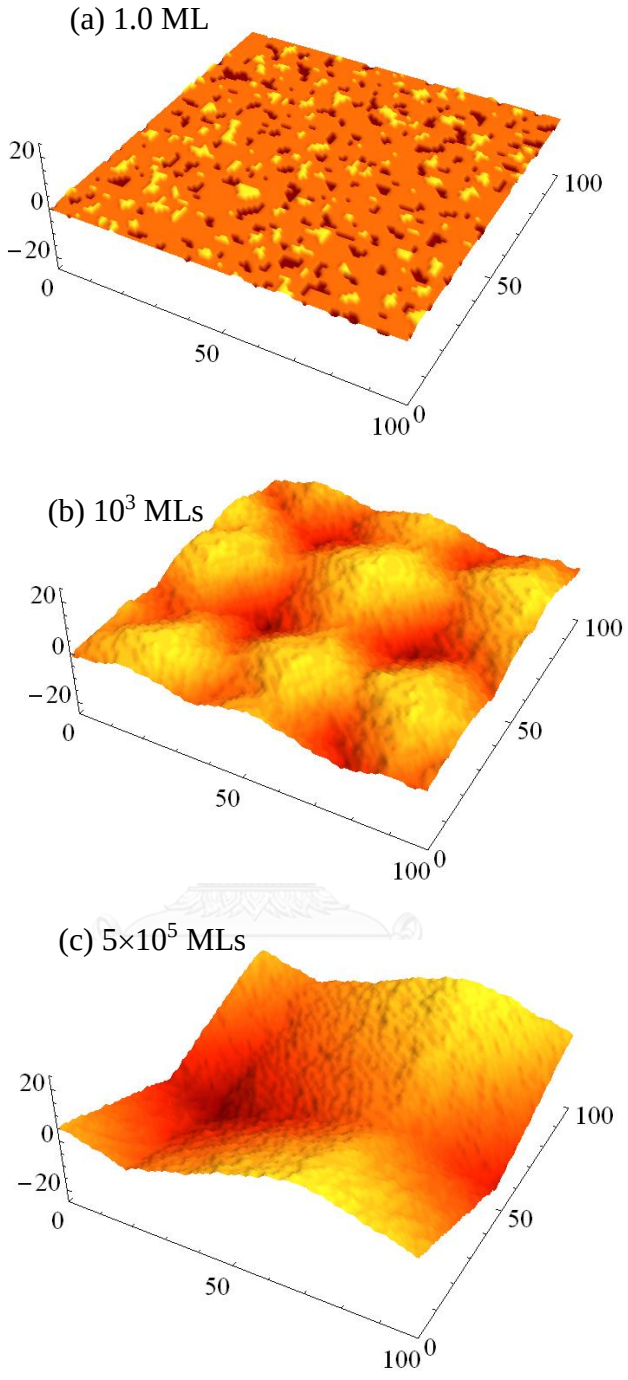

Fig. 3. 6 Surface morphologies of the WV model with the $m = 1$ and $\ell = 25$ at t (a) 1.0 MLs (b) 1.0×10^3 MLs, and (c) 5.0×10^5 MLs

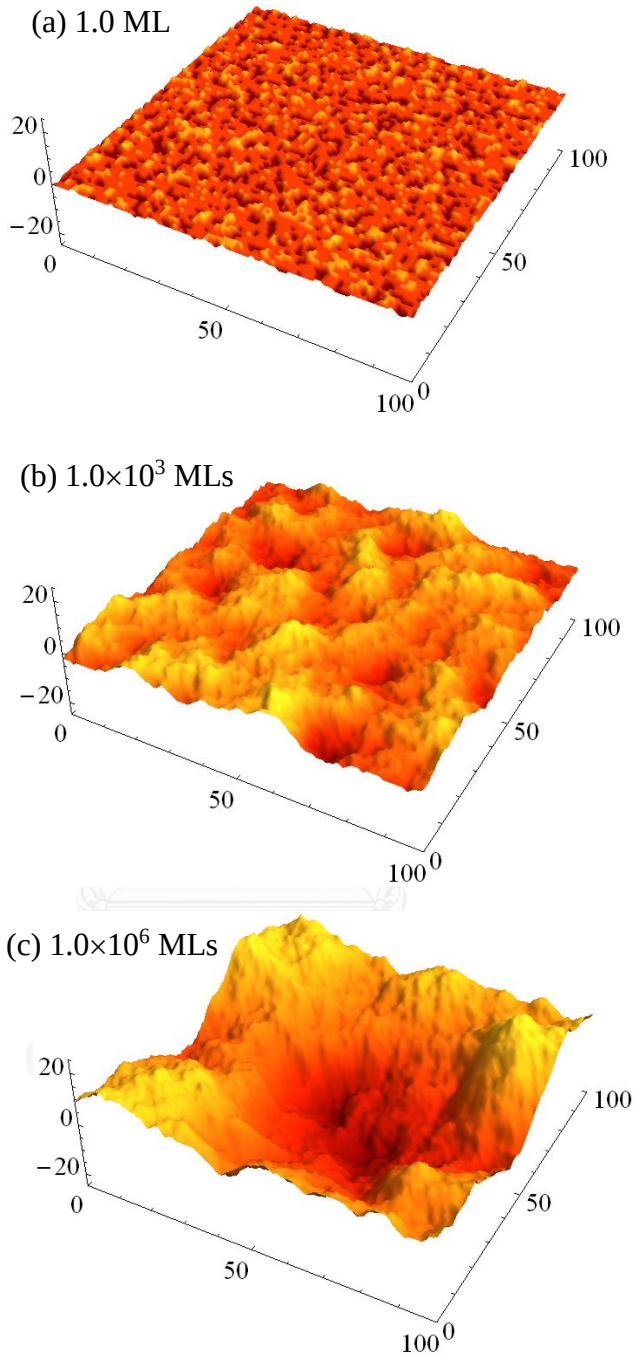

Fig. 3. 7 Surface morphologies of the LC model with m = 1, $\ell = 1$ at t (a) 1.0 MLs (b) 1.0×10^3 MLs, and (c) 1.0×10^6 MLs

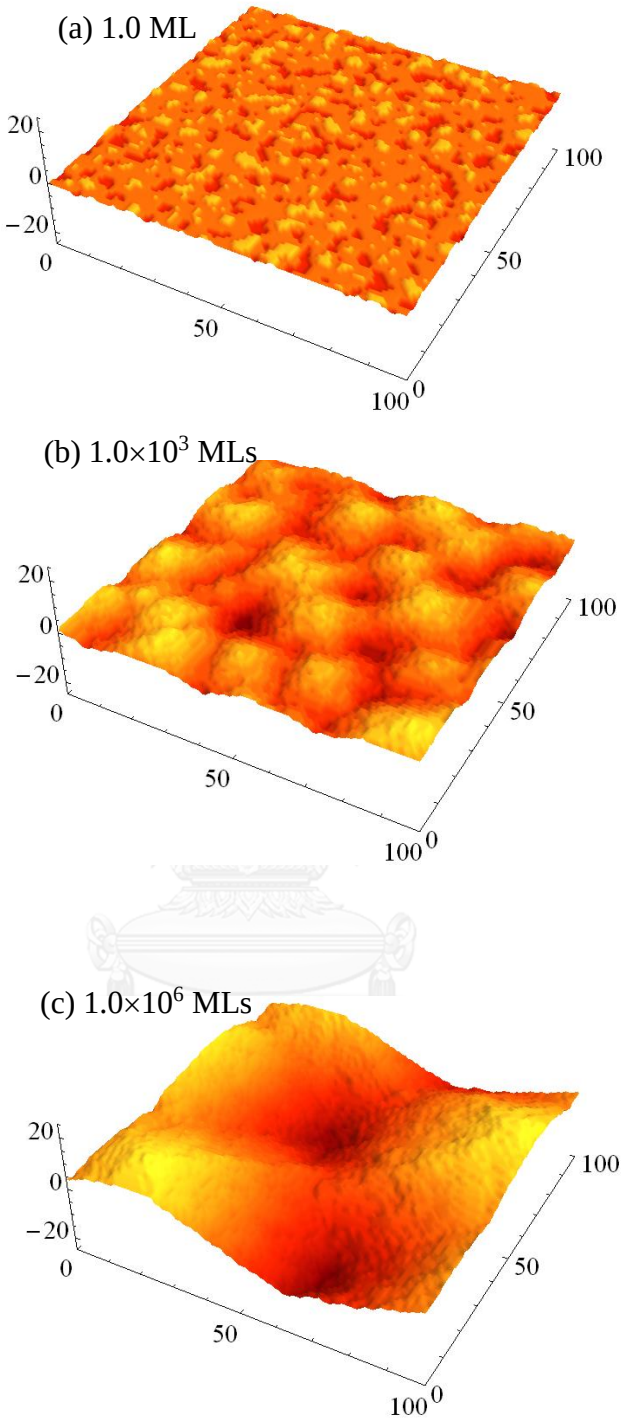

Fig. 3. 8 Surface morphologies of the LC model with $m = 5$, $\ell = 1$ at t (a) 1.0 MLs (b) 1.0×10^{3} MLs, and (c) 1.0×10^{6} MLs

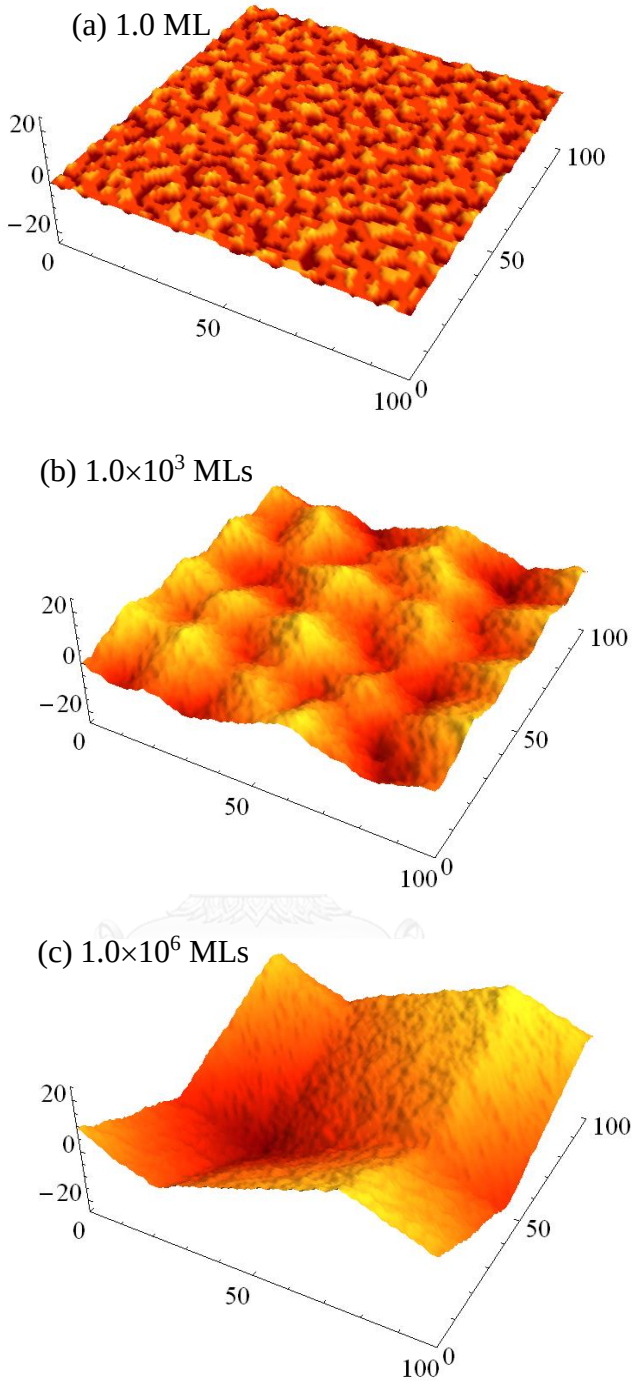

Fig. 3. 9 Surface morphologies of the LC model with $m=1$, $\ell=25$ at t (a) 1.0 MLs (b) 1.0×10^{3} MLs, and (c) 1.0×10^{6} MLs

when $\ell \geq 5$ for the $\ell > 1$ NRT. The mounding of the noise reduced LC model arises from the SED instability caused by the uphill current which have been described in Ref. [26]. In addition, our morphology results agree with previous work [26] and also complete the mounding study in epitaxial growth as shown in Ref. [26] and [28].

Finally, the F model which is in the EW class described by Eq. 2.3. The morphology grown with the F model is smoother than the film simulated with other models. Fig. 3.10(a) shows the surface from the original F ($m = 1$ and $\ell = 1$) and Fig. 3.10(b) and 3.10(c) present the noise reduced F model. We can see that when the noise is reduced with m (Fig. 3.10 (b) and with ℓ (Fig. 3.10 (c)), the morphologies become very smooth.

3.2 Effects of the NRTs on the interface width and the growth exponent

In this section, effects of the NRTs on interface width, and the growth exponent are investigated. The value of L is 100 throughout the chapter except when the effect of the substrate size is investigated and L is varied (Fig. 3.19 in section 3.2.2). All models are simulated up to the steady state. The results from the films grown with the DT, WV, and LC models will be shown only.

3.2.1 Interface width of the DT, WV, and LC models with and without the NRTs

The effects of the noise reduction parameters (m and ℓ) on the interface width are investigated. Plots of W versus t the growth models with the NRTs are presented.

In order to study effects of the $m > 1$ NRT, plots of $W(t)$ for the DT model with the $m > 1$ NRT is shown in Fig. 3.11. The oscillations indicating layer-by-layer growth can clearly be observed in early time. They become damp and eventually disappear at later time when the interface width crossover to kinetically rough region. This same behavior is seen in both the WV (Fig. 3.12), and the LC (Fig. 3.13) models, in agreement with previous works [17, 18, 27, 38].

The oscillation of W reveals that each layer is grown from a flat surface, then the surface width increases until a layer is half filled. The film becomes a flat surface at a completely filled layer before the next layer is grown. Thus the interface width

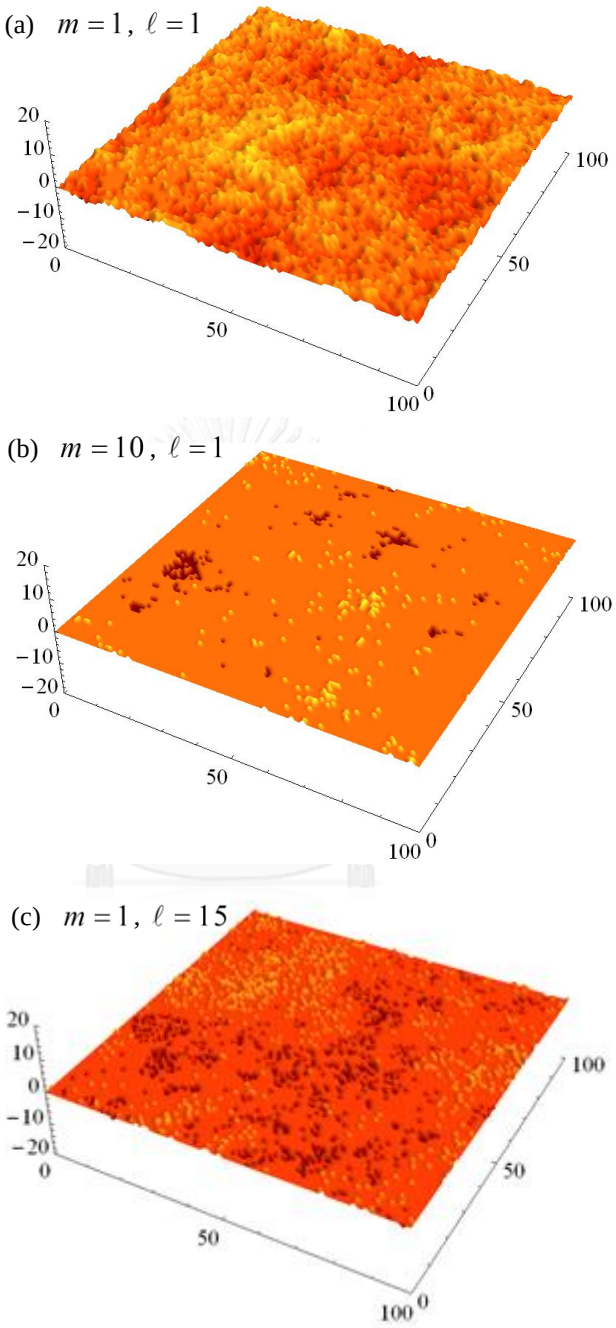

Fig. 3. 10 Surface morphologies of the F model when (a) $m=1$ and $\ell=1$, (b) $m=10$ and $\ell=1$, and (c) $m=1$ and $\ell=15$ in the steady state at 10^5 MLs.

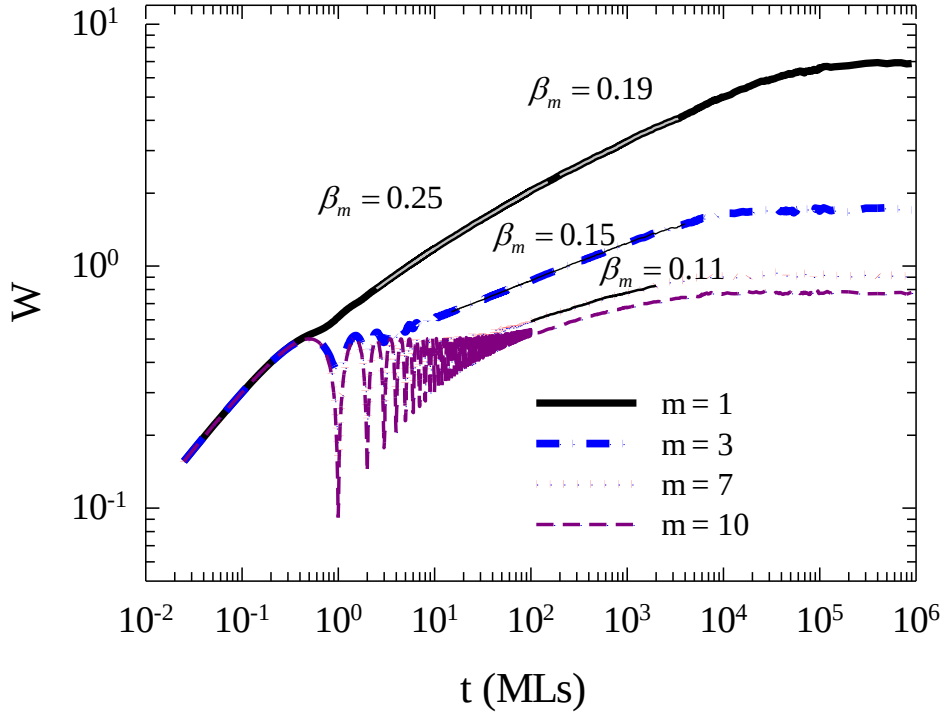

Fig. 3. 11 Plots of $W(t)$ for the DT model, $\ell = 1$, and m = 1, 3, 7,and 10. The growth exponents correspond to the best slope fit.

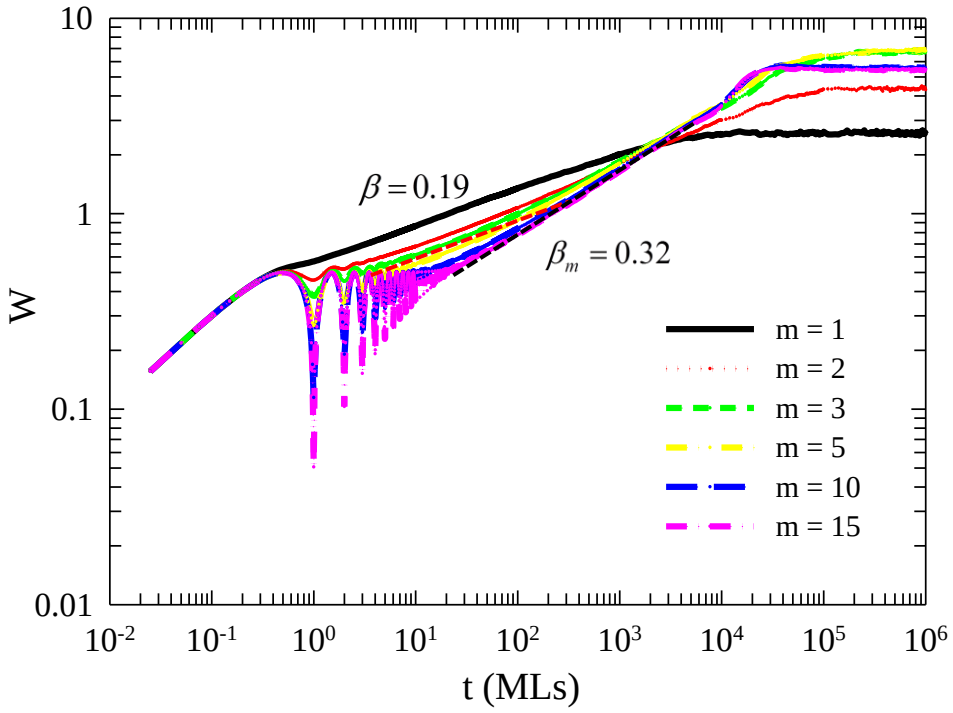

Fig. 3. 12 Plots of $W(t)$ for the WV model when $\ell = 1$, and m = 1, 2, 3, 5, 10, and 15. The growth exponents correspond to the best slope fit.

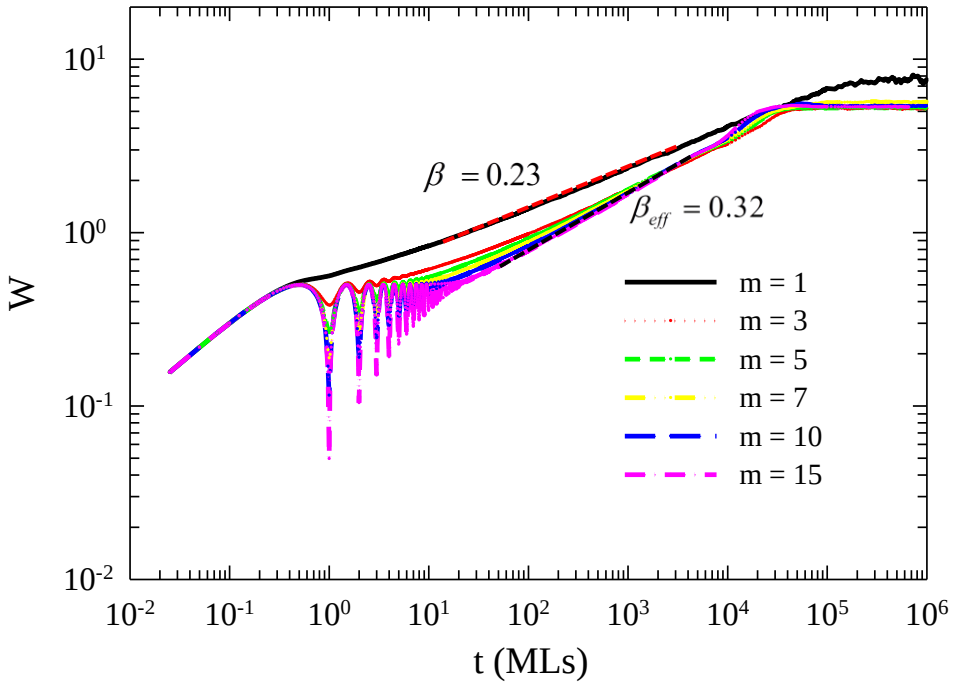

Fig. 3. 13 Plots of $W(t)$ for the LC model when $\ell = 1$, and m = 1,3, 5, 7, 10, and 15. The growth exponents correspond to the best slope fit.

fluctuates between the minimum values (a filled layer) and the maximum values (a half filled layer) and a period of the oscillations is one monolayer (ML). Note that, for "perfect" layer-by-layer growth, W fluctuates between 0 (a completely filled layer) and 1 (a half completely filled layer).

The W oscillations are damped because a new layer starts forming before the preceding layer is completely filled. Thus W is not reduced to zero. Consequently, our results show that $m>1$ NRT yields layer-by-layer growth at the beginning of the growth process for all models studied here.

In the $\ell>1$ NRT, the damped oscillations of $W(t)$ for the DT (Fig. 3.14) and WV (Fig. 3.15) models are observed when the noise is reduced with parameter ℓ. The oscillations are obviously observed when parameter ℓ is increased. These results agree with the effects from the $m>1$ NRT. However, the damped oscillation is not seen in the $W(t)$ plot for the LC model. This means that, unlike the $m>1$ NRT, the $\ell>1$ NRT does not induce layer-by-layer growth in the LC model (see Fig. 3.16). Investigation of the morphologies shows that mound formation develops from the beginning of the growth process (seen in Fig. 3.8).

At later growth time, our morphologies confirm that both $m>1$ and $\ell>1$ NRTs promote very smooth surface in the DT model (seen in Fig. 3.3) and mound formation in the WV (Fig. 3.4 - 3.6) and LC (Fig. 3.7 - 3.9) models.

3.2.2 Effects of the NRTs on the growth exponent of the DT, WV, and LC models

Next, we study effects of the noise reduction parameters (m and ℓ) on the growth exponent (β) of the DT, WV, and LC models. We found that the noise reduced growth exponents β_m and β_m, which are the exponent obtained using different noise reduction parameters m and ℓ, depend quite strongly on the value of m and ℓ when they are small. However, for large m and ℓ, β_m and β_ℓ do not change much as shown in Fig. 3.17 - 3.18.

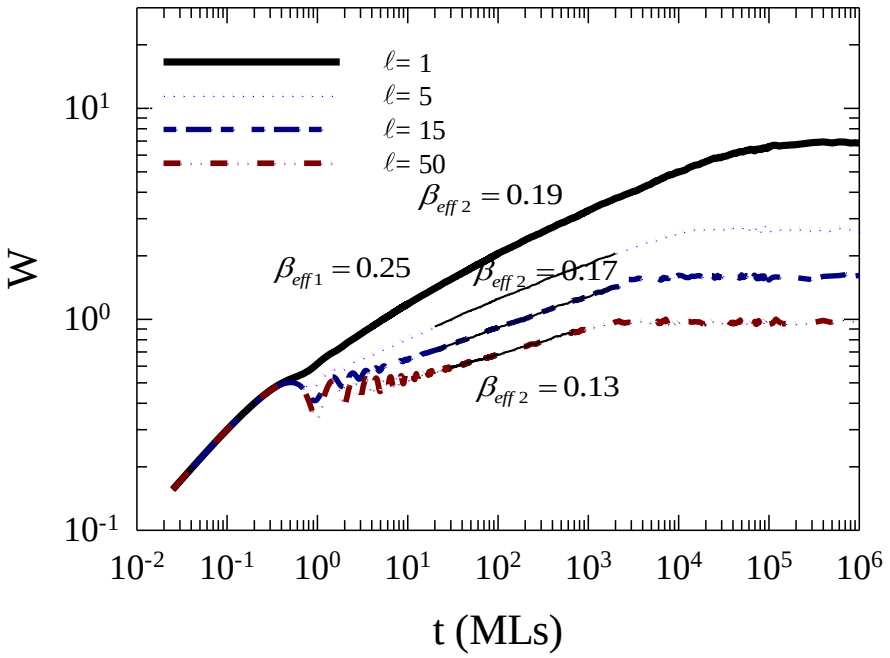

Fig. 3. 14 Plots of $W(t)$ for the DT model when $m = 1$, and ℓ = 1, 5, 15,and 50. The growth exponents correspond to the best slope fit.

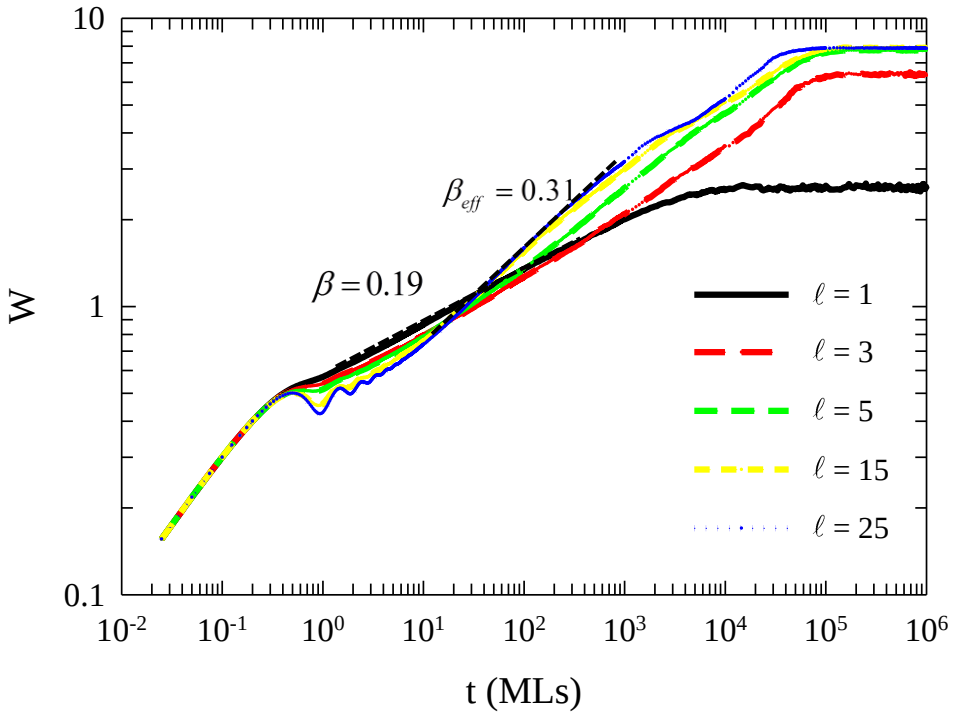

Fig. 3. 15 Plots of $W(t)$ for the WV model when $m = 1$, and ℓ = 1,3, 5, 15, and 25. The growth exponents correspond to the best slope fit.

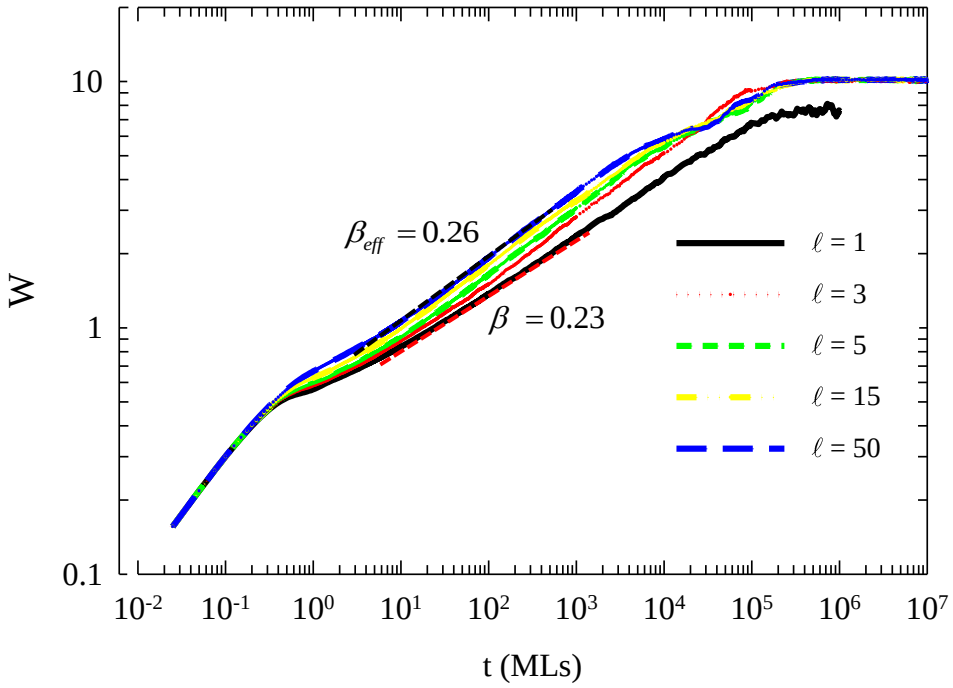

Fig. 3. 16 Plots of $W(t)$ for the LC model when $m = 1$, and ℓ = 1, 3, 5, 15, and 50. The growth exponents correspond to the best slope fit.

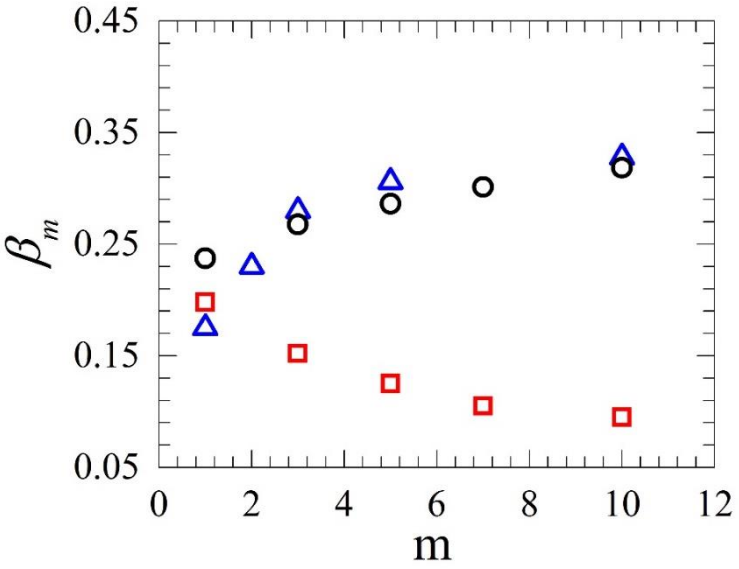

Fig. 3. 17 Plots of β_m versus m for the DT (square), WV (triangle), and LC (circle) models when $L=100$ and $\ell=1$.

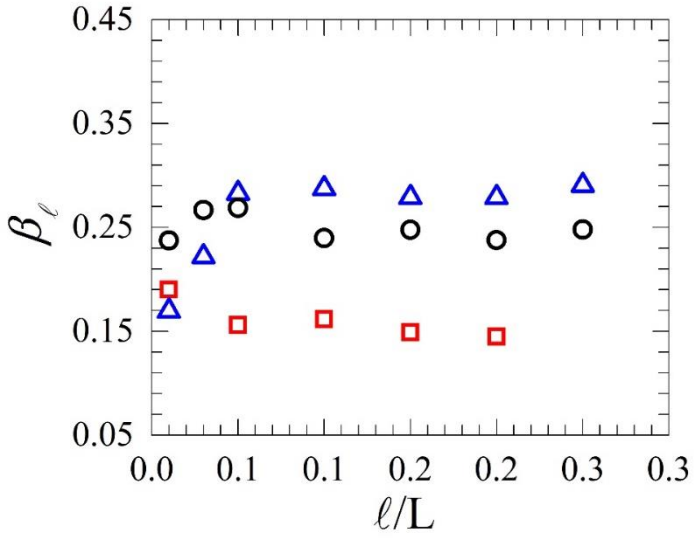

Fig. 3. 18 Plots of β_ℓ versus ℓ / L for the DT (square), WV (triangle), and LC (circle) models, when $L=100$ and $m=1$.

In the original DT model ($m=1$and $\ell=1$), during early time ($t<10^2$ MLs), the best fit yields $\beta_{(1)}=0.25$ while in the later time ($t>10^2$ MLs), the best fit provides $\beta_{(2)}=0.19$ as shown in Fig. 3.11 and Fig. 3.14. The value $\beta_{(1)}=0.25$ is close to the theoretical calculation from the MH class in Eq. 2.5. This is not the true asymptotic value for the growth exponent for the DT model [17, 22]. The value $\beta_{(2)}=0.19$ during later growth time is very close to the theoretical value from the VLDS class in Eq. 2.15. However, we can suggest that the growth exponent for the (2+1) DT model is approximately 0.2, in agreement with previous works [17, 22]. Consequently, the crossover shows that the continuum equation describing the DT model contains both [40] the linear forth-order term $(\nabla^4 h)$ and the nonlinear fourth-order term $(\nabla^2(\nabla h)^2)$.

In order to study the effects of noise reduction, we can see that when m is increased, β_m decreases to $\beta_m \approx 0.10$ at $m=10$ (the DT model in Fig. 3.17). At large ℓ, β_ℓ also decreases to $\beta_\ell \approx 0.13$ (the DT model in Fig. 3.18). The decreasing of β_m and β_ℓ for large m and ℓ hints at the possibility of a crossover to the EW universality class which has been shown to be the asymptotic universality class of the (2+1) DT model.

In the WV model, the value of the growth exponent is 0.2 when $m=1$and ℓ=1, which is consistent with previous works [33, 37]. When m and ℓ are increased, β_m and β_ℓ both increase significantly (see Fig 3.17 and Fig. 3.18). At the largest m and ℓ used here, both β_m and β_ℓ become larger than 0.3 which does not agree with any known universality classes. It is possible that the calculation of the growth exponent may not be of much use in the model with mounded morphologies.

For the LC model, $\beta \approx 0.25$ when $m=1$and ℓ=1 indicating that the (2+1) LC model belongs to the MH universality class as it should be. However, when m is increased (see Fig. 3.17), we found that β_m increases in exactly the same way as in the noised reduced WV model. So, we can suggest that the noise reduction parameter m yields decreasing growth exponent and provides $\beta \geq 0.3$ for mounded surface grown with the WV and LC models. Additionally, increasing ℓ (see Fig. 3.18), on the other

hand, does not have much effect on the growth exponent as the value of β_ℓ remains $\beta = 0.25$ for all ℓ used here.

In Fig. 3.19, we show our results of the effective growth exponent in all 3 models with $\ell > 1$ NRT, denoted $\beta_{\ell,eff}$. For each ℓ , $\beta_{\ell,eff}$ is obtained by calculating β_ℓ from systems with different substrate size L, plotting β_ℓ as a function of $\frac{1}{L}$, then extrapolate the curve for $\beta_{\ell,eff}$ which is β_ℓ as $L \to \infty$ as shown in Fig. 3.20. Fig. 3.20 is the plot of β_ℓ when $L =$ 50, 100, 150, 200, and 250 for the DT model with $\ell = 10$. From the plot, $\beta_{\ell,eff} \approx 0.16$ for the DT model with $\ell = 10$. This extrapolation is done in an attempt to reduce the finite size effect on β_ℓ. For this plot, the value of L ranges from 50 to 250. It can be seen that Fig. 3.20, although not identical to Fig. 3.18, offers approximately the same information: increasing ℓ leads to the slow decrease of β_ℓ in the DT model, significant increase of β_ℓ in the WV model, and not much change in β_ℓ in the LC model.

Our results shown in this section suggest that studying the growth exponent may not be the best method to determine the asymptotic universality of the DT, WV, and LC models because of the crossover. However, the results obtained indicate that the $m > 1$ NRT yields similar behavior in the WV and LC models.

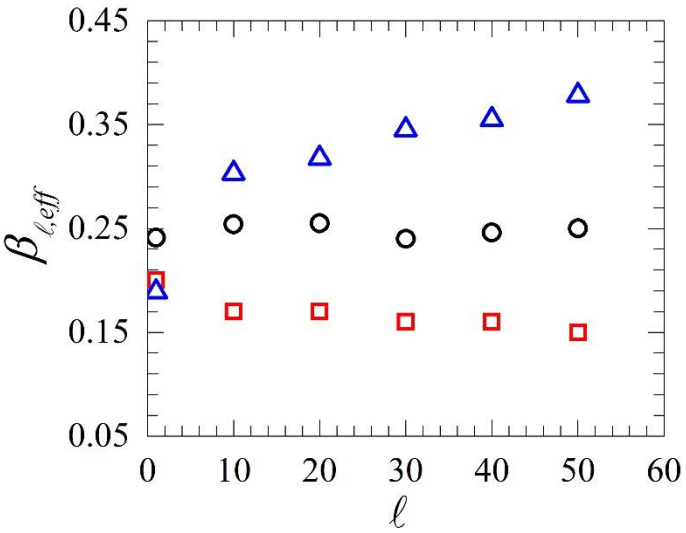

Fig. 3. 19 Plots of $\beta_{\ell,eff}$ versus ℓ for the DT (square), WV (triangle), and LC (circle) models when $m=1$.

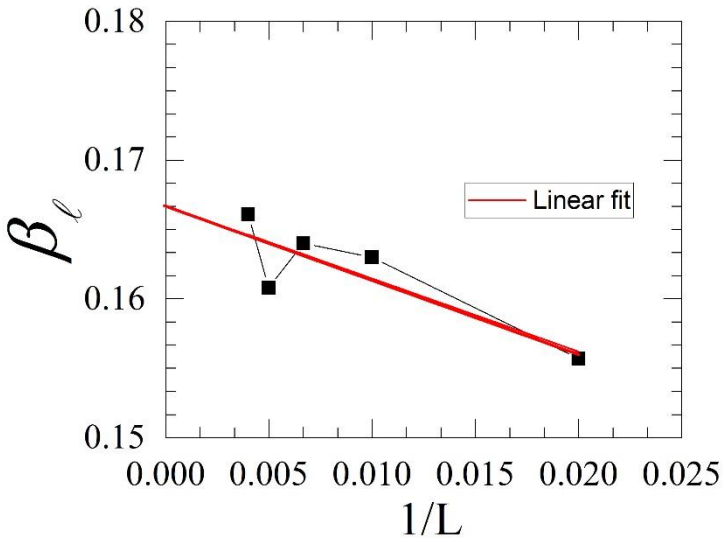

Fig. 3. 20 Plots of β_ℓ versus 1/L for the DT when $\ell=10$ and L= 50, 100, 150, 200, and 250.

CHAPTER IV

RESULTS AND DISCUSSIONS: ROUGHNESS DITRIBUTION

In chapter III, conventional method for finding universality class are shown. In this chapter, the roughness distributions and its quantitative characterization such as skewness and kurtosis of the original BD, DT, WV, LC, and F models will be shown. Effects of the NRTs on the roughness distribution on the DT, WV and the LC are presented. Finally, effects of substrate size on the noise reduced DT, WV, and LC models will be presented. In this chapter, value of L is 100 throughout the chapter except when effect of the substrate size is investigated and L is varied (in section 4.3).

4.1 Roughness distributions of growth models without the NRTs

The roughness distributions at the steady state are studied for the (2+1)-dimensional BD, DT, WV, LC, and F models. The roughness distribution in Eq. (2.11), along with S and Q in Eq. (2.14) and (2.15) are calculated.

Fig. 4.1 - 4.5 show the roughness distributions of the original BD, DT, WV, LC, and F models. In the graph, the distributions are calculated using $N \approx 9\times10^8$ (for the BD, DT, WV and F models) and $N \approx 10^9$ (for the LC model). From the roughness distribution of each model, S and Q are calculated. We obtained $S \approx 1.6$ and $Q \approx 5.1$ for the BD model, in agreement with previous works [10, 14]. For the DT model, we found $S \approx 1.1$ and $Q \approx 2.1$. The closest theoretical values of S and Q are from the VLDS universality class [10]. Roughness distribution of the WV model has $S \approx 1.0$ and

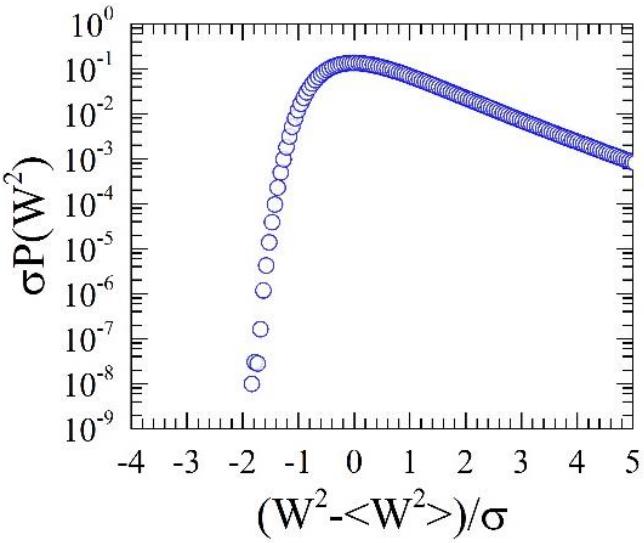

Fig. 4. 1 Roughness distribution of the BD model with $m=1$ and $\ell=1$.

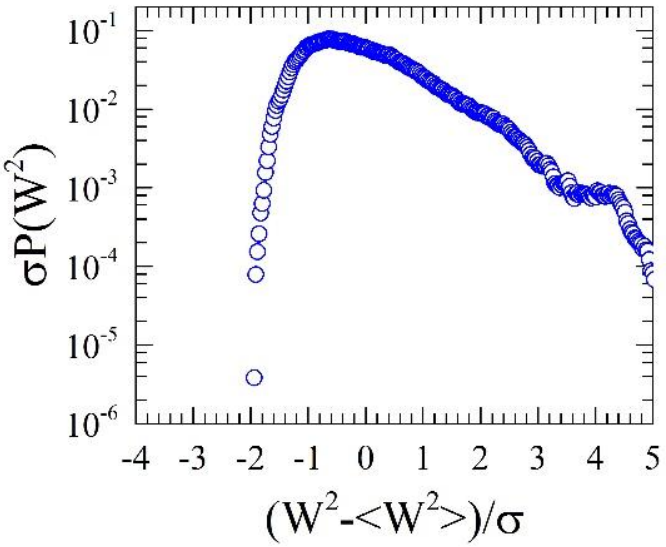

Fig. 4. 2 Roughness distribution of the DT model with $m=1$ and $\ell=1$.

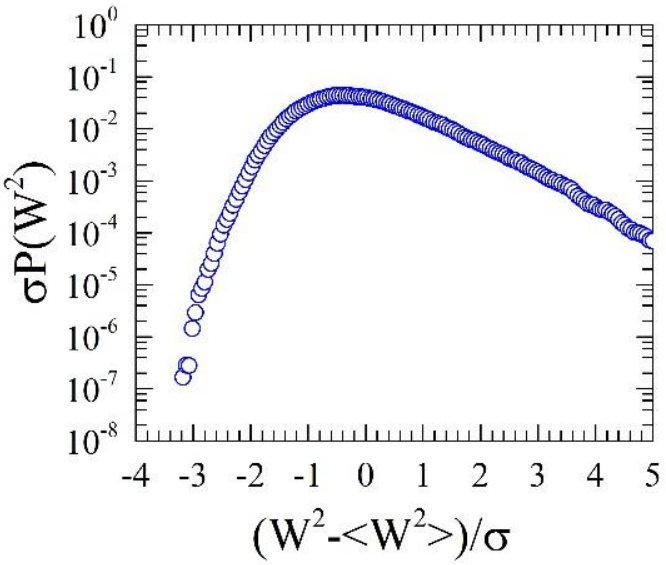

Fig. 4. 3 Roughness distribution of the WV model with $m=1$ and $\ell=1$.

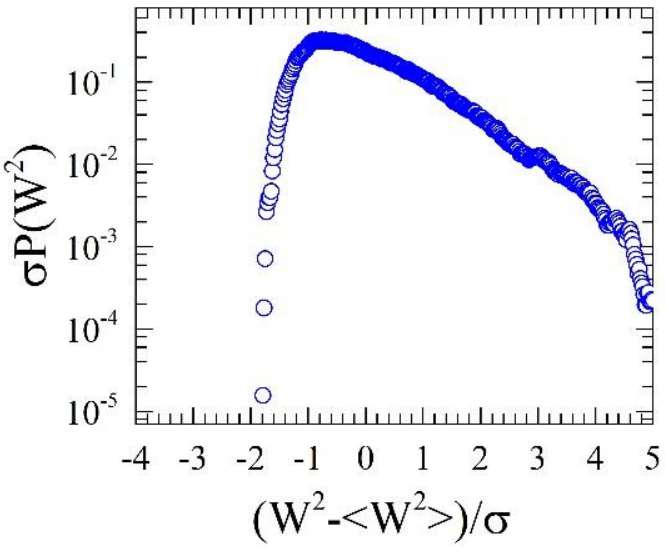

Fig. 4. 4 Roughness distribution of the LC model with $m=1$ and $\ell=1$.

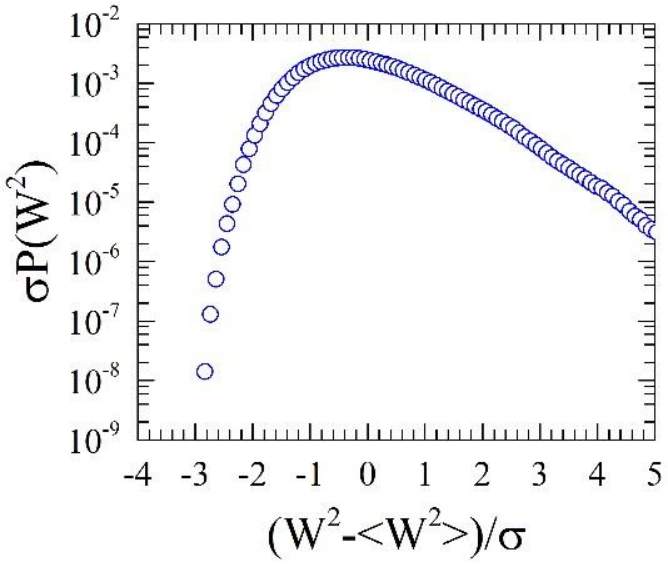

Fig. 4. 5 Roughness distribution of the F model with $m=1$ and $\ell=1$.

$Q\approx 1.9$, which also agree approximately with the VLDS class. For the LC model, we obtained $S\approx 1.3$ and $Q\approx 2.3$. These values are close to the theoretical values of the MH universality class [10]. In the F model, we obtained $S\approx 0.6$ and $Q\approx 0.9$.

4.2 Roughness distributions of growth models with the NRTs

In this part, the noise is reduced with the parameter m and ℓ to investigate roughness distribution of the growth models. For the DT model, Fig. 4.6 shows the roughness distribution when the parameter m is increased from $m=1$ (original model) to $m=10$. It is clear that the roughness distribution does not change significantly with the noise reduction parameter m. The values of S and Q do not change much either. We found $S\approx 1.1$ and $Q\approx 2.1$ in the original model, while $S\approx 1.0$ and $Q\approx 1.9$ when $m=10$. The $\ell>1$ NRT leads to similar results with insignificant change in the roughness distribution curve (see Fig. 4.7). The film grown with the largest ℓ used here, $\ell=50$, yields $S\approx 1.2$ and $Q\approx 2.1$. These S and Q agree approximately with the theoretical values of $S\approx 1.1$ and $Q\approx 1.8$ in the VLDS class [10]. These results seem to indicate that both NRTs, within the limit of m and ℓ used here, still do not lead to

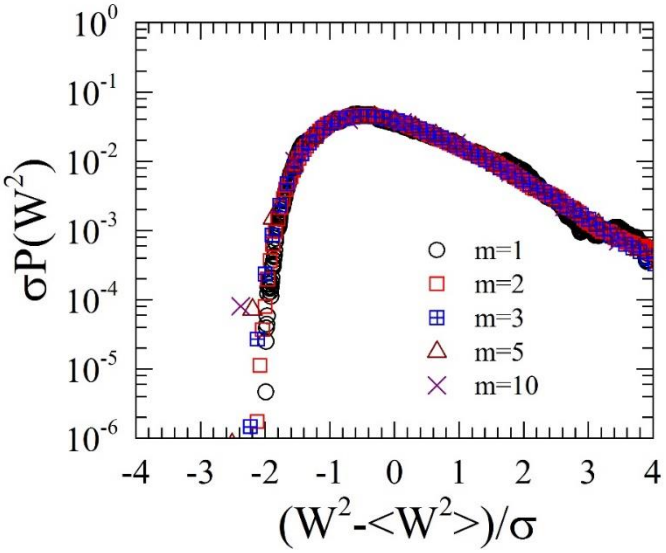

Fig. 4. 6 Roughness distributions of the DT model with the $m > 1$ NRT.

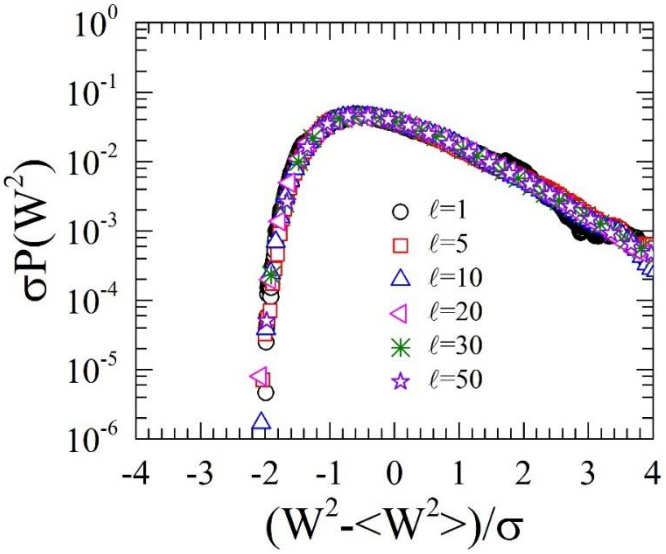

Fig. 4. 7 Roughness distributions of the DT model with the $\ell > 1$ NRT.

roughness distribution curve of the expected EW distribution [8]. The cause of this discrepancy maybe the finite size effects as shown in Ref. [21] for the (1+1)-dimensional DT model.

In the WV model, the NRTs drastically affect the roughness distribution curve of the WV model. Fig. 4.8 presents the roughness distributions for the WV with the $m>1$ NRT. We obtained that when m is large enough to induce mounded morphologies, the roughness distribution turns into a normal distribution. At $m=10$, we obtained $S\approx 0.1$ and $Q\approx 0.2$. The WV model with the $m>1$ curves can be fitted with the Gaussian function,

$$f(x)=ae^{\left[-c\left(\frac{x-x_0}{b}\right)^2\right]}, \tag{4.1}$$

with $a=0.24$, $b=1$, $c=0.5$, and $x_0=-0.019$. Similar shift of the roughness distribution to the Gaussian curve is found in the WV model with $\ell>1$ NRT. Fig. 4.9 shows the roughness distributions for the WV with $\ell>1$ NRT. At $\ell=50$, we obtained $S\approx 0.0$ and $Q=0.0$. The $\ell>1$ curves can be also fitted with the Gaussian function, with $a=0.03$, $b=1$, $c=0.5$, and $x_0=-0.008$.

In the LC model, the NRTs lead to roughness distribution which can be fitted with the Gaussian function as well. The distribution curves, with $m>1$ NRT, are presented in Fig. 4.10. The solid line is the Gaussian fit using $a=0.12$, $b=0.96$, $c=0.5$, and $x_0=-0.05$. We obtained the skewness and kurtosis of the distribution at $m=10$ as $S\approx 0.2$ and $Q\approx 0.2$. The distribution, with $\ell>1$, are shown in Fig. 4.11. The solid line shows the Gaussian fit using $a=0.3$, $b=1$, $c=0.5$, and $x_0=-0.007$. Both S and Q are approximately zero at $\ell=50$.

4.3 Effects of substrate size on the roughness distribution

In this part, effects of the substrate size on the roughness distributions of the three models with the NRTs are investigated. When the substrate size is varied, we found that the roughness distributions are statistically unchanged as shown in Fig 4.12. Fig 4.12 (a) shows the DT model with $m=5$ when the substrate size, L, is varied from 80, 100, 130, to 200. The roughness distribution curves of all substrate sizes collapse

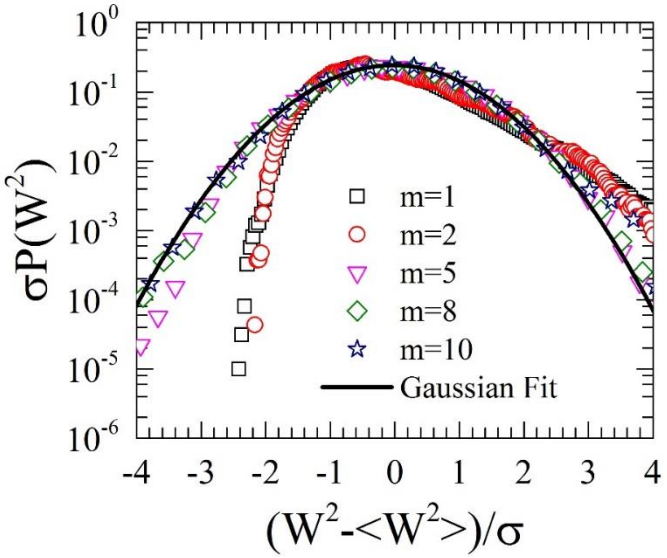

Fig. 4. 8 Roughness distributions of the WV model with the $m > 1$ NRT. Solid line shows the fit obtained with the Gaussian function.

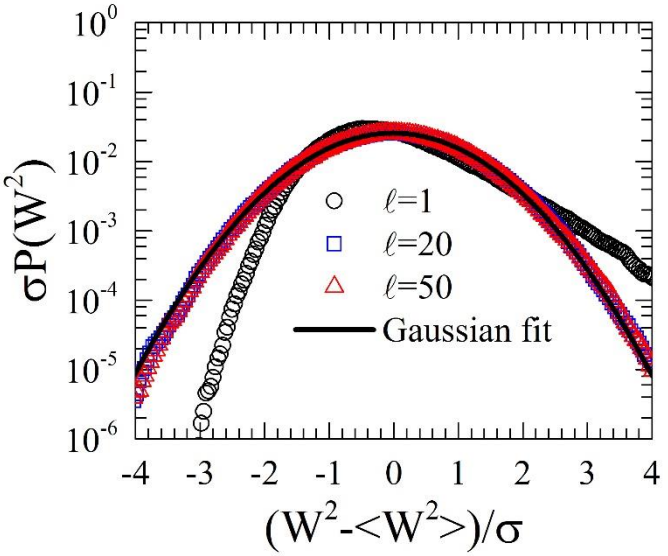

Fig. 4. 9 Roughness distributions of the WV model with the $\ell > 1$ NRT. Solid line shows the fit obtained with the Gaussian function.

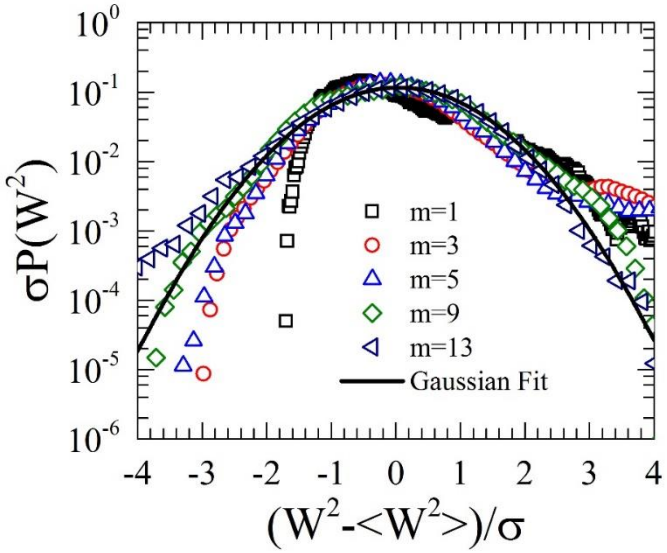

Fig. 4. 10 Roughness distributions of the LC model with the $m>1$ NRT. Solid line shows the fit obtained with the Gaussian function.

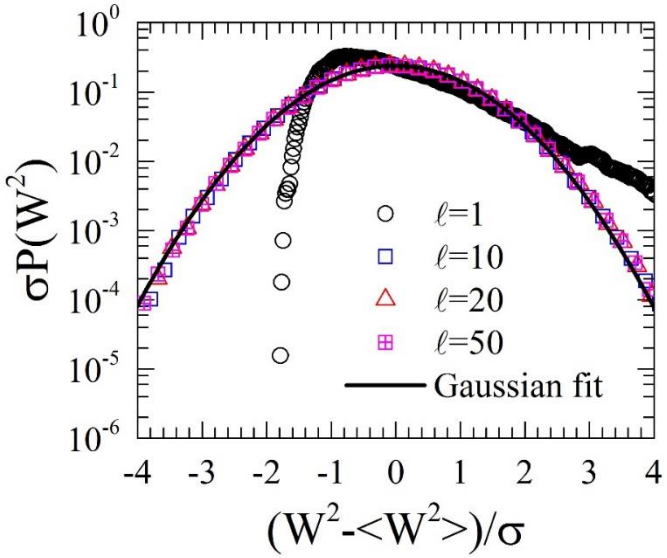

Fig. 4. 11 Roughness distributions of the LC model with the $\ell>1$ NRT. Solid line shows the fit obtained with the Gaussian function.

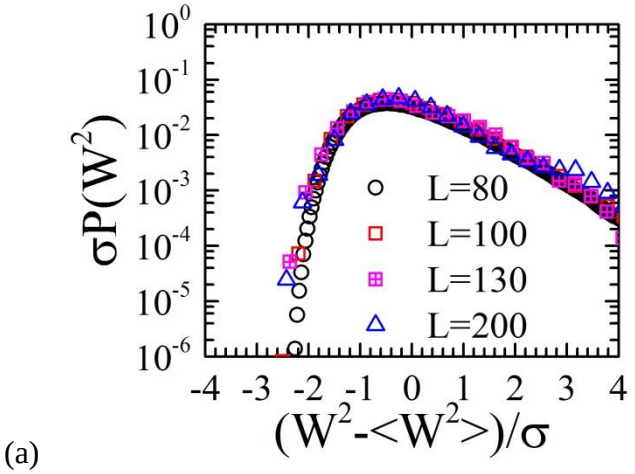

(a)

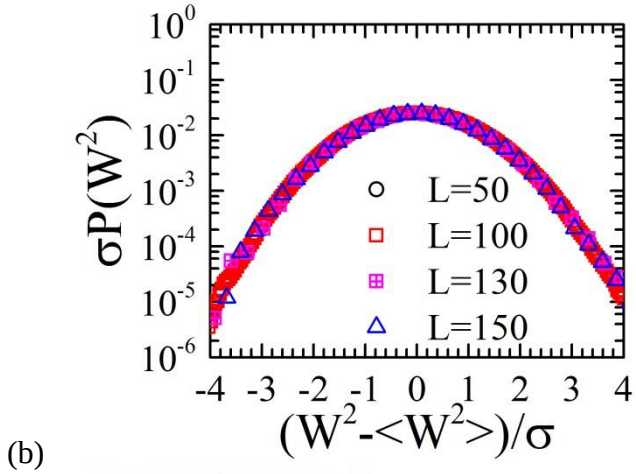

(b)

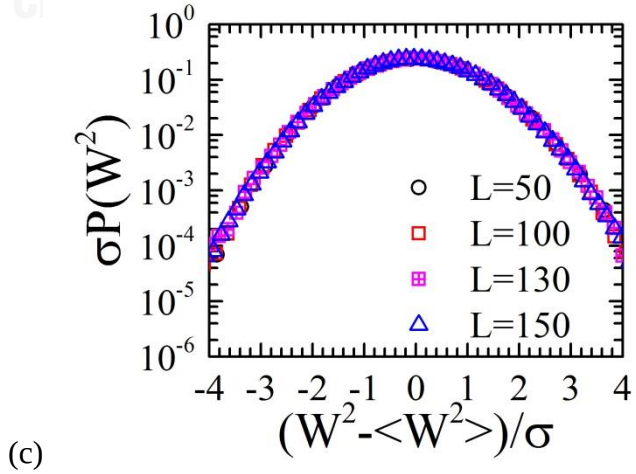

(c)

Fig. 4. 12 Roughness distributions of the (a) DT model ($m = 5$), (b) WV model ($\ell = 20$), and (c) LC model ($\ell = 20$) using various substrate sizes.

into the same curve. This confirms that the substrate size does not affect the roughness distribution of the DT model with the $m>1$ NRT. Similar results are obtained for the WV and the LC models with the $\ell>1$ NRT. Fig 4.12 (b) and Fig 4.12 (c) are the roughness distributions of the $\ell>1$ WV and LC models respectively. For both models, the diffusion length used in these plots is $\ell=20$. The substrate size is varied from 50, 100, 130, to 150. Similar to the $m>1$ NRT cases, all roughness distribution curves collapse into the same normal distribution curve. Similar results are obtained for the DT model with the $\ell>1$ NRT.

According to our results, the values of S and Q for all 3 models, both original and with NRTs, are summarized in Table 1. Note that the theoretical values of the skewness and kurtosis (in (2+1)-dimensional films) for the distribution curves of the MH are $S\approx 1.30$ and $Q\approx 2.63$ [10] while $S\approx 1.1$ and $Q=1.8$ for the VLDS distribution [10].

The results found in the original models are not surprising, but the noise reduced results are quite remarkable. Actually, we expected to see a slow change in the noise reduced DT roughness distribution from the VLDS to the EW class and the LC roughness distribution curve to remain the same, as the LC model, by construction, is purely MH class. However, our results are completely different. The NRTs do not change anything in the DT model, but lead to the change of the roughness distribution curves of both WV and LC models to ones that can be fitted beautifully with the Gaussian function and negligible S and Q. In the case of the DT model, it is possible that we do not see any change because the finite size effects may keep the DT roughness distribution in the shape of the VLDS class. As for the noise reduced WV and LC models, both of them have mounded morphologies when the noise reduction factor is large enough and the saturated mounded morphologies of the two models are almost indistinguishable. Although unexpected, it may be reasonable for the roughness distribution, calculated directly from the saturated morphologies, of the two models to be the same as well. We note also that, although previous works [17, 26, 38] have shown that the NRTs do not change asymptotic behavior of growth models, our findings here show the possibility that the universality class of the models may be affected.

Table 1 The values of S and Q for the BD, DT, WV, LC, and F models with and without NRTs.

Model	$m=1, \ell=1$		$m=10, \ell=1$		$m=1, \ell=50$	
	S	Q	S	Q	S	Q
BD	≈ 1.6	≈ 5.1	-	-	-	-
DT	≈ 1.1	≈ 2.1	≈ 1.0	≈ 1.9	≈ 1.2	≈ 2.1
WV	≈ 1.0	≈ 1.9	≈ 0.1	≈ 0.2	≈ 0.0	≈ 0.0
LC	≈ 1.3	≈ 2.3	≈ 0.2	≈ 0.2	≈ 0.0	≈ 0.0
F	≈ 0.6	≈ 0.9	-	-	-	-

CHAPTER V

RESULTS AND DISCUSSIONS: HEIGHT DISTRIBUTION

In this chapter, time varying height distributions of the growth models with and without the NRTs are simulated. The height distributions are investigated both in the early time and the steady state were presented. Beside, finite size effects on the height distribution are also shown. In this part, result shown are from simulation film on substrates of size $L \times L$ lattice sites. Value of L is $L = 100$ except when an effect of the substrate size is investigated and L is varied (in section 5.3).

.

5.1 Skewness and kurtosis of the height distribution in the early time

5.1.1 The LC, DT, and WV models with the multiple hit NRT

In the LC model, when the $m > 1$ NRT is applied, the film is grown in the layer-by-layer at early time indicated by the oscillating of the interface width (see Fig. 3.13). The oscillations become damp and eventually disappear at later time (less than 30 MLs). For example, if $m = 15$, interface width crossover to kinetically rough region at 30 MLs. The layer-by-layer growth is near perfect at larger m.

To study the height distribution of the layer-by-layer growth, time varying S and Q of the height distribution are investigated. The calculated S and Q are shown in Fig. 5.1. Morphologies at very early time are shown in Fig. 5.2.

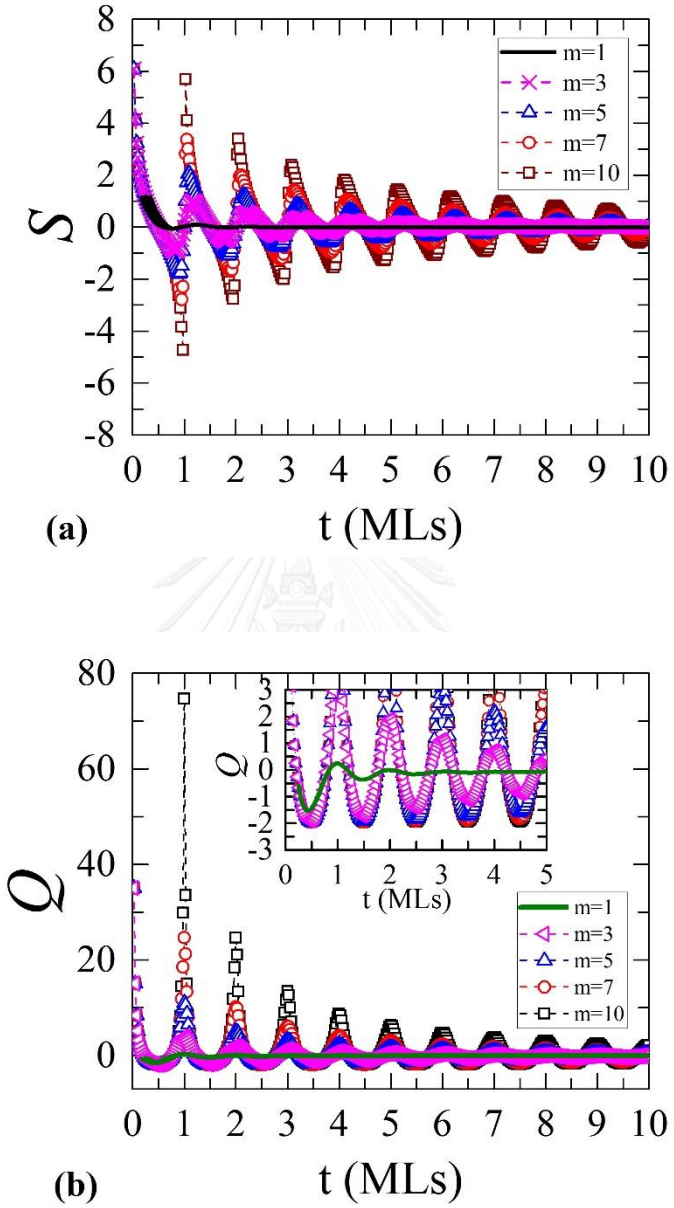

Fig. 5. 1 Plots of (a) S and (b) Q versus t at early growth time of the LC model with the $m>1$ NRT

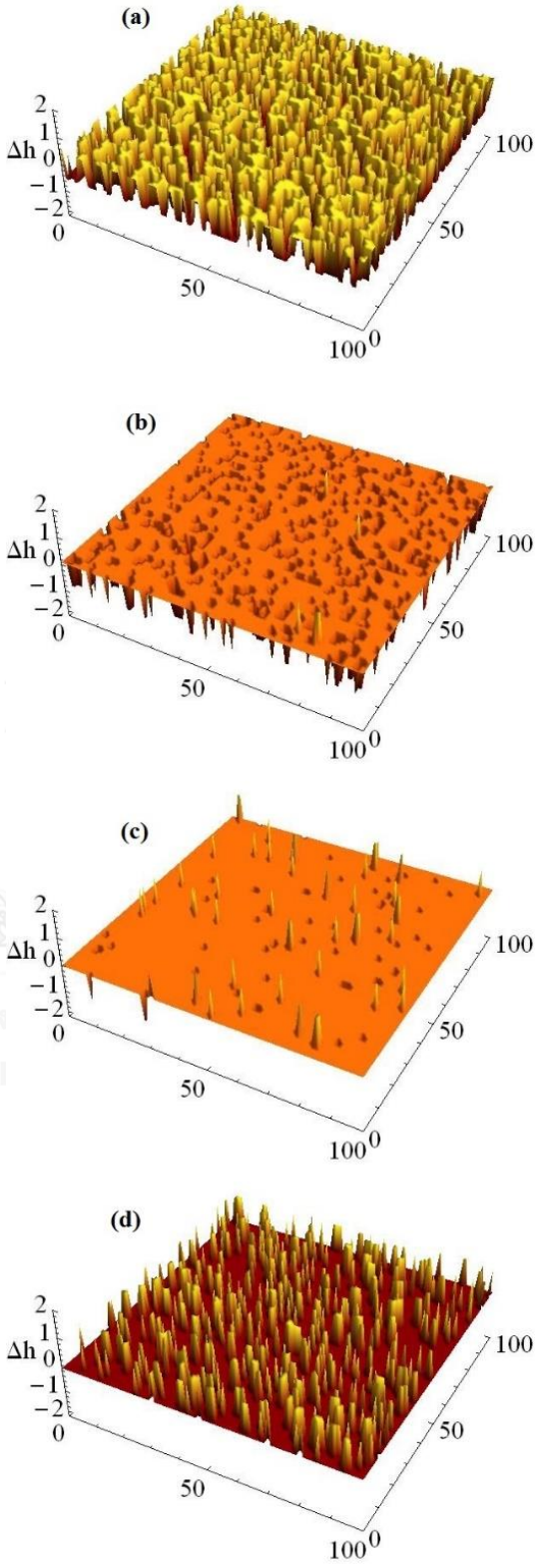

Fig. 5. 2 Surface morphologies of the LC model when $\ell = 1$ and $m = 10$; (a) at 0.5 ML (b) at 0.9 ML (c) at 1.0 ML, and (d) at 1.1 ML.

In Fig 5.1(a), at early growth time (less than 10 MLs), the S value fluctuates between the maximum and the minimum values when $m > 1$. Period of the oscillations is one monolayer (ML). Amplitudes of the oscillations become larger as m is increased, which corresponds to a near-perfect layer-by-layer growth. From Fig. 5.1(a), S gradually decreases from $S = 0$ at 0.5 ML to its minimum value before abruptly jumps back to $S = 0$ at 1.0 ML. It then rises rapidly to its maximum value before gradually decreases to $S = 0$ at 1.5 ML. This complete one cycle of the oscillation of S. Figs. 5.2(a) - (d) show morphologies when the noise is reduced with $m = 10$. Fig. 5.2(a) shows the morphology at 0.5 ML when $S = 0$ (as seen in Fig. 5.1(a)). The zero of S indicates that the number of sites that have higher and lower height than the average value are the same. This result agrees with the up-down symmetric morphology in Fig 5.2(a). Fig. 5.2(b) shows the surface with a very large negative S at 0.9 ML. It is clear that the height fluctuations (Δh) are either zero or negative. The film at 0.9 ML is obviously negatively skewed. Fig. 5.2(c) illustrates the surface at 1.0 ML which shows up-down symmetry. A film at 1.1 ML is shown in Fig. 5.2 (d). It is obvious that the surface is positively skewed in this case.

Note that although the values of S at 0.5 ML and 1.0 ML are both zero, their surface morphologies (Fig. 5.2(a) and Fig. 5.2(c) are not similar. The reason is that even when the height of most positions on the surface at 0.5 ML are varied, the numbers of the positions with height lower and higher than 0.5 ML are equal as shown in Fig. 5.2(a). On the other hand, the height fluctuation of most sites on surface at 1 ML is zero and the surface is quite smooth.

Fig. 5.1(b) shows the oscillation of $Q(t)$ of the LC model when the $m > 1$ NRT is incorporated with the inset showing details of the curves. We find that Q oscillates with period 1 ML as well. At 0.5 ML, the value of Q is at its minimum negative value which corresponds to the morphology in Fig. 5.2(a). The height of each site on the surface is varied so the height distribution is broad. After that, the value of Q gradually increases to the maximum positive value at $t \approx 1.0$ ML. The height of most sites are the same and the surface becomes quite smooth as shown in Figs. 5.2(b) – (d).

Additionally, S and Q values can be used to quantitatively analyze the surface morphologies as shown in Figs. 5.2(a) to (d). For example, if $S = 0$ and $Q = -2.0$ (see

Fig.5.2 (a)), the surface has up-down symmetry and the height of each site on the film are varied, whereas $S = -2.6$ and $Q = 5.1$ (see Fig. 5.2(b)) indicate that the height of most sites on the surface are higher than the height average and the top of the surface is smooth. In Fig. 5.2(c) ($S = 0$ and $Q = 80.3$), the surface has up-down symmetry and the film is very smooth. In Fig. 5.2(d) ($S = 2.7$ and $Q = 5.1$), most positions on the surface are smaller than the height average and the surface is smooth.

In conclusion, we find that S and Q values can be used to quantitatively analyze the surface morphologies. When $S = 0$ and $Q < 0$, the morphology is rough with up-down symmetry (Fig. 5.2(a)), however if $S = 0$ but $Q > 0$, the film is smooth with up-down symmetry (Fig. 5.2(c)). When $S < 0$ and $Q > 0$, the film is smooth with tiny grooves (Fig. 5.2(b)) while $S > 0$ and $Q > 0$ indicates a smooth morphology with tiny pillars (Fig. 5.2(d)).

The DT model with the $m > 1$ NRT is also studied for comparison. $W(t)$ of the noise reduced DT model oscillates during small t when the noise is reduced. $S(t)$ and $Q(t)$ oscillations of the DT model with the $m > 1$ NRT are presented in Fig. 5.3(a) and 5.3(b). The period of the oscillations is 1 ML. At a half monolayer, we found that $S = 0$ and $Q < 0$, while at every complete layer $S = 0$ and $Q > 0$. Our DT results are consistent with the LC results.

Finally, we also study the roughness distribution of the WV model when the noise is reduced with m. The $m > 1$ NRT induces the layer-by-layer growth same as the LC and DT results. Then $W(t)$ becomes damped oscillation as shown in Fig. 3.12. Time varying height distribution presented in Fig. 5.4(a) and 5.4(b) also agree with the LC (see Fig. 5.1) and DT (see Fig. 5.3) results.

5.1.2 The LC and DT models with the long surface diffusion length NRT

We investigate the height distribution of the $\ell > 1$ LC model. Noise reduction parameter; $\ell = 1$, 3, 5, 10, 15, and 50 are used. In the early growth time ($t \leq 100$ MLs), we found that the $\ell > 1$ NRT does not lead to layer-by-layer growth as with the $m > 1$ NRT (see Fig. 3.16). This is evident by the study of the interface width which does not

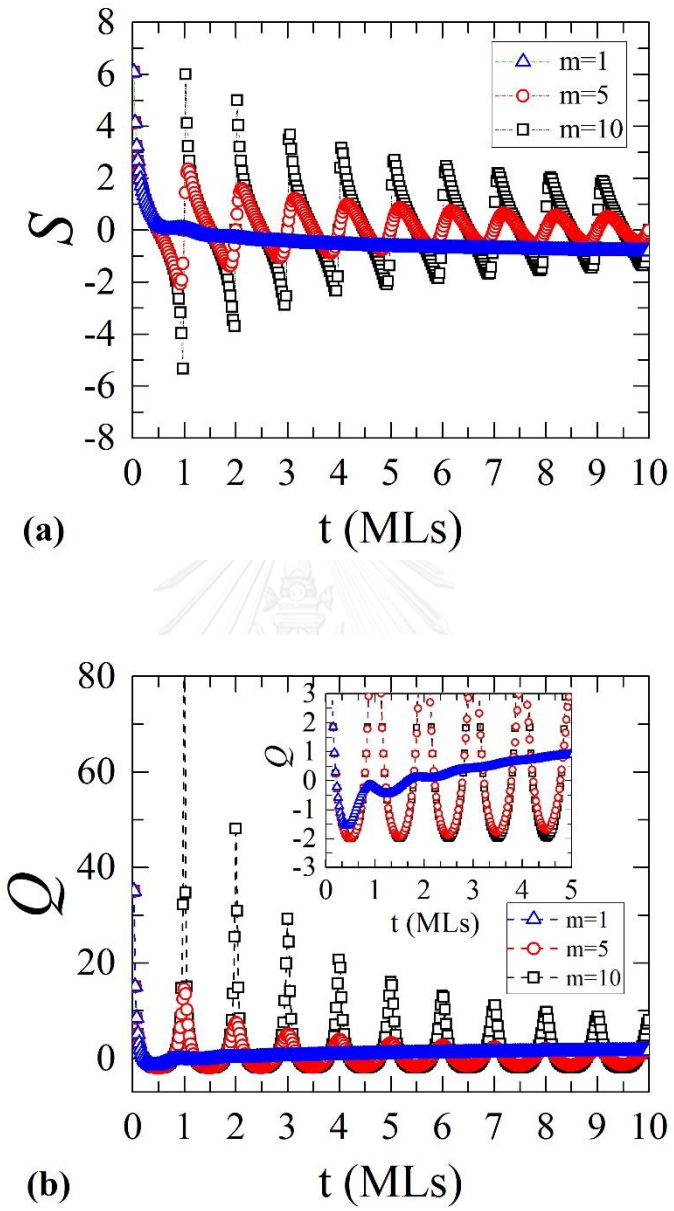

Fig. 5. 3 Plots of (a) S and (b) Q versus t at early growth time of the DT model with the $m>1$ NRT.

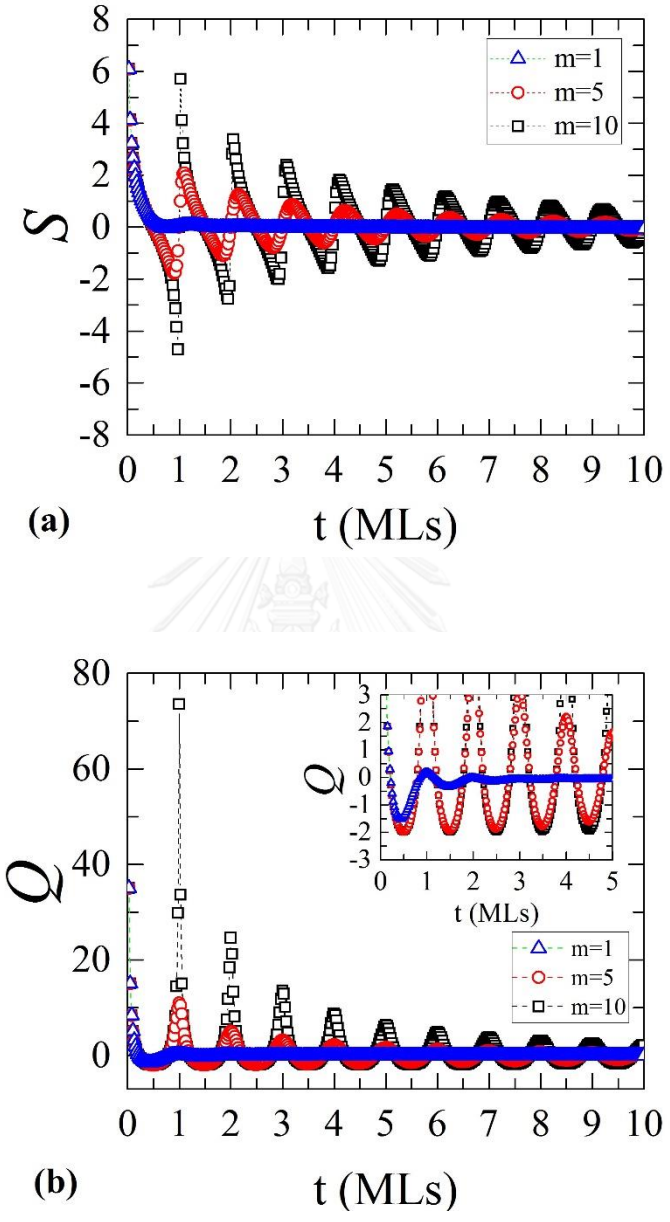

Fig. 5. 4 Plots of (a) S and (b) Q versus t at early growth time of the WV model with the $m>1$ NRT.

show any oscillation for any value of ℓ. These results are confirmed by plots of $S(t)$ in Fig. 5.5(a) and $Q(t)$ in Fig. 5.5(b). It is clear from the plots that when ℓ is increased, the small oscillation of S and Q, which are observed only in the first ML, sharply decreases. This means that the layer-by-layer growth is interrupted and it eventually disappeared, which agree with morphology result. At beginning growth time (≈ 1 ML), the film becomes mounded surface instead of smooth surface.

The $S(t)$ and $Q(t)$ of the DT model with the $\ell > 1$ NRT is studied to compare the results with those of the LC model. The $\ell > 1$ NRT induces the layer-by-layer in the DT model (seen in Fig. 3.14) and the $S(t)$ and $Q(t)$ results presented in Fig. 5.6(a) and 5.6(b) agree with the results from the DT model with the $m > 1$ NRT.

5.2 Skewness and kurtosis of the height distribution in the steady state

5.2.1 The LC, WV, and DT models with the multiple hit NRT

Surface morphologies in the steady state of the $m > 1$ LC, WV, and DT models are studied. The $m > 1$ NRT leads to a perfect single mounded morphology as illustrated in Fig. 5.7. In Figs. 5.7(a) - (d), the mounded surfaces of the LC model in the steady state are illustrated, here the noise is reduced with $m = 1$, 3, 5, and 10. The $m > 1$ NRT leads to a single mound on the saturated film for all values of m used here. Fig. 5.8 shows the scaled height distributions corresponding to the morphologies in Fig. 5.7. Note that the scaled height distributions from systems with different m are approximately the same. This is expectable since the saturated morphologies of different m do not differ. Fig. 5.8 is the scaled height distributions of the $m \geq 1$ LC model. A solid line is the Gaussian fit. We can see that all scaled height distributions in Fig. 5.8 are nearly the same.

Fig. 5.9 shows the values of S and Q with various m. It can be seen that S fluctuates around $S \approx 0$ while Q is negative and almost constant for all m. Our finding that S is approximately zero indicates that the mounded morphologies obtained from the $m > 1$ LC model are also approximately up-down symmetric. The $m > 1$NRT does not affect the up-down symmetric property of the LC model. The negative values of Q

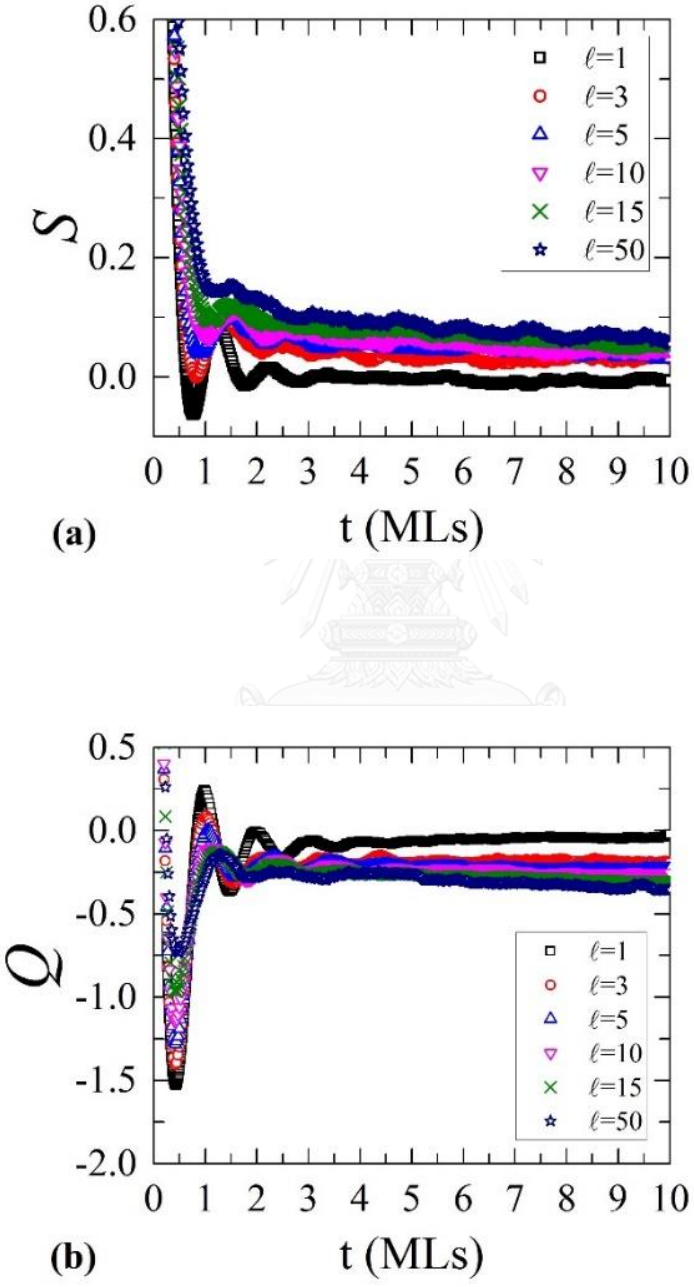

Fig. 5. 5 Plots of (a) S and (b) Q versus t at early growth time of the LC model with the $\ell > 1$ NRT.

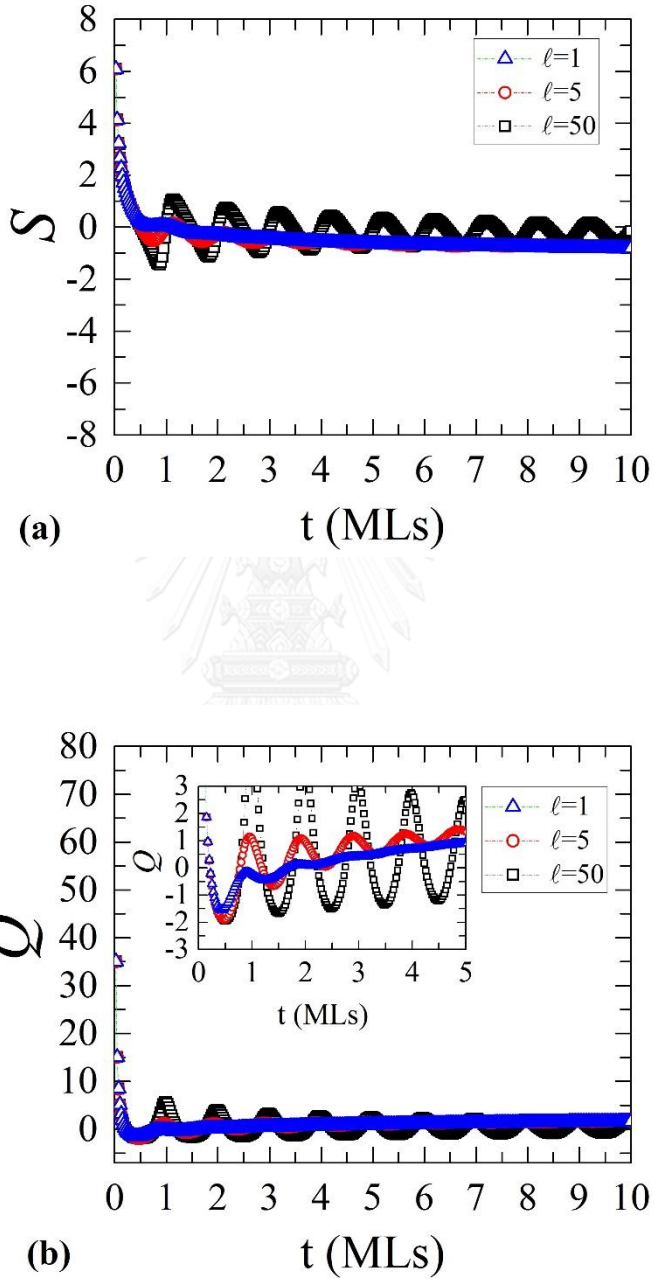

Fig. 5. 6 Plots of (a) S and (b) Q versus t at early growth time of the DT model with the $\ell > 1$ NRT.

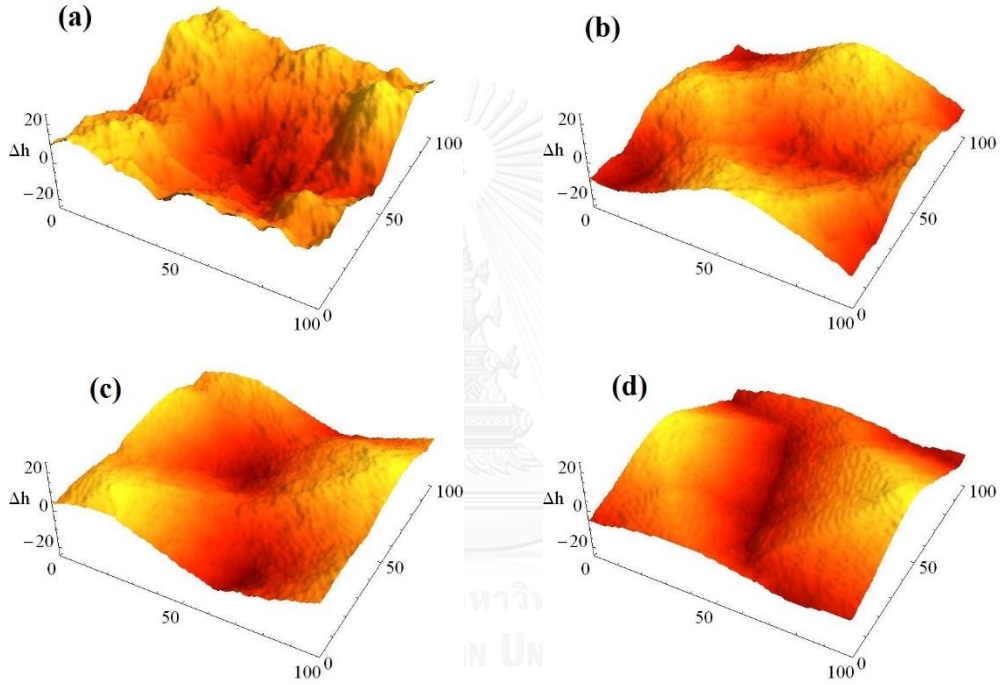

Fig. 5. 7 Surface morphologies of the $m > 1$ LC model at the steady state with (a) $m = 1$ (at 1×10^{6} MLs), (b) $m = 3$ (at 1×10^{5} MLs), (c) $m = 5$ (at 1×10^{5} MLs), and (d) $m = 10$ (at 1×10^{5} MLs).

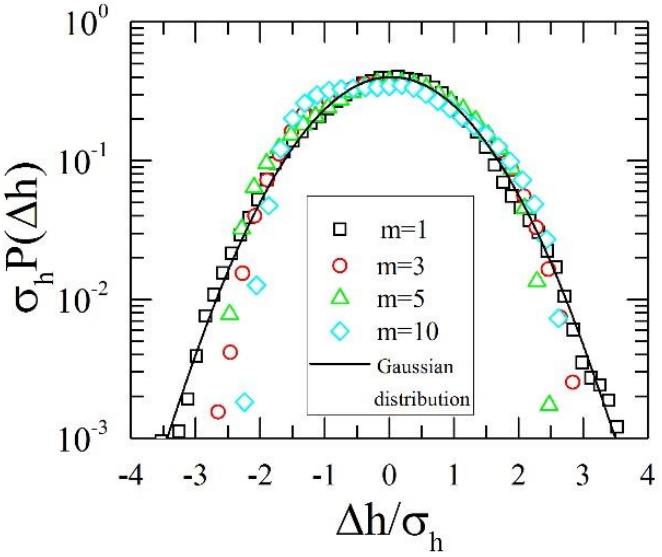

Fig. 5. 8 Plots of the height distribution at the steady state of the LC model with the $m > 1$ NRT.

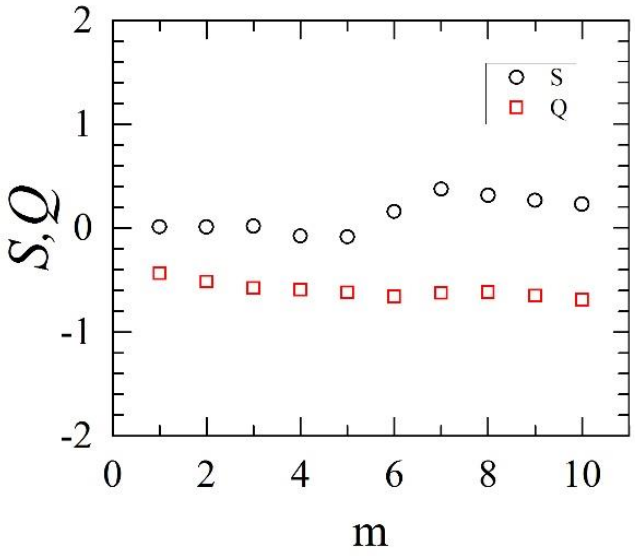

Fig. 5. 9 Plots of S and Q of the height distribution at the steady state of the LC model with the $m > 1$ NRT.

indicates that the single mounded morphology is rough and the $m>1$ NRT does not change the roughness of the film.

In the WV model, the skewness and kurtosis are $S=-0.06\pm0.03$ and $Q=-0.16\pm0.04$. The value of skewness shows an up-down symmetry of the surface. When m is increased (see Fig. 5.10), we found that S is approximately zero same as the LC result. This imply that a single mounded surface grown with the $m>1$ WV model are approximately up-down symmetric. Moreover, the value of Q is slightly decreases from $Q\approx-0.2$ at m =1 to $Q\approx-1.0$ at $m=10$. This indicates that the single mounded morphology is rough and the $m>1$ NRT does not change the roughness of the film.

The height distribution of the DT model is also studied. The surface morphologies in the steady state of the $m>1$ DT model (seen in Fig. 3.3(b) and 3.3(c)) present that the $m>1$ NRT leads to a smooth morphology. In the original DT model, the skewness and kurtosis of height distribution are $S=-0.66\pm0.04$ and $Q=1.4\pm0.2$. From the values of S and Q, we found that when m is increased the skewness increases and converts to zero and the kurtosis decrease to zero as illustrated in Fig. 5.11. This indicates that the height distribution of the $m>1$ DT model becomes the normal distribution at large m.

5.2.2 The LC, WV, and DT models with the long surface diffusion length NRT

Surface morphologies at the steady state of the $\ell>1$ LC, WV, and DT models are investigated. The values of ℓ used here are $\ell=1$, 3, 5, 10, 15, 25, and 50 for the LC model and $\ell=1$, 5, and 50 for the WV and DT models.

We found that the $\ell>1$ NRT leads to a single mounded morphology in the LC and WV models (seen in Fig.3.9 (c) and Fig. 3.6 (c) respectively). When $\ell>1$, the height distributions of the LC and WV models are slightly changed confirmed by the plots of the S and Q in Fig. 5.12 (for the LC model) and in Fig. 5.13 (for the WV model). We found that the values of S and Q do not change significantly when the $\ell>1$ NRT is applied to the LC and WV models. This indicates that the $\ell>1$ NRT

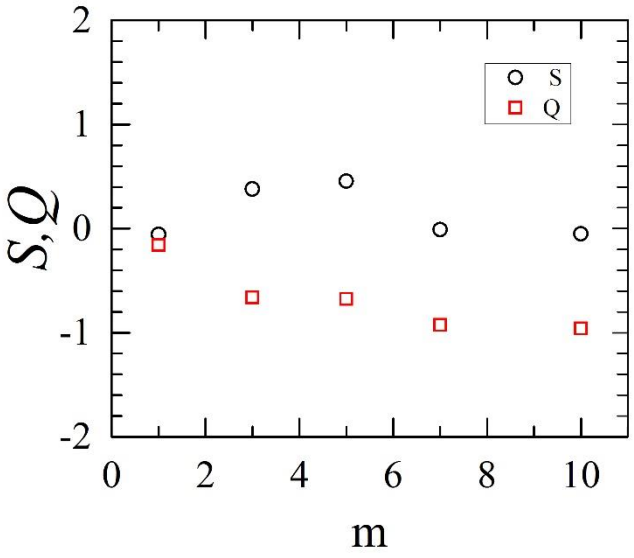

Fig. 5. 10 Plots of S and Q of the height distribution at the steady state of the WV model with the $m>1$ NRT.

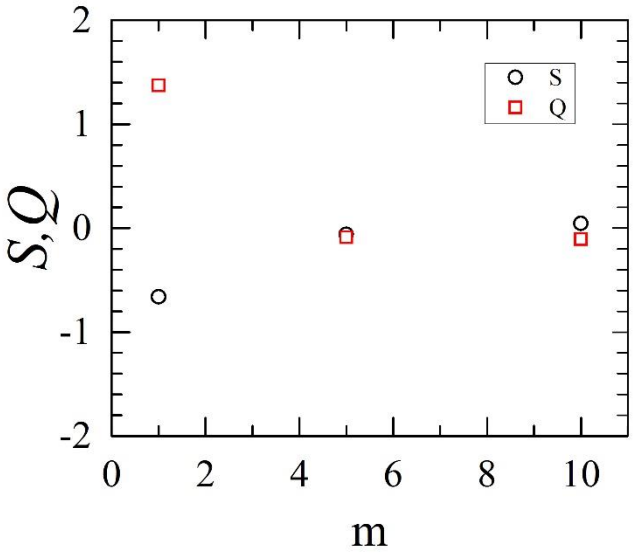

Fig. 5. 11 Plots of S and Q of the height distribution at the steady state of the DT model with the $m>1$ NRT.

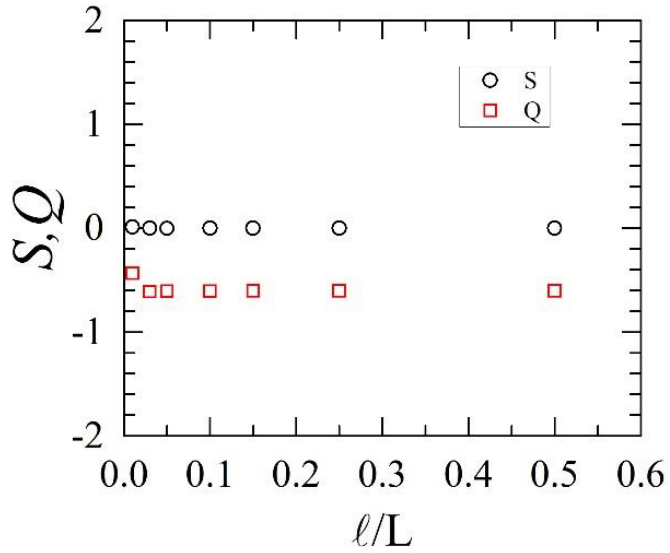

Fig. 5. 12 Plots of S and Q at the steady state for the LC model with the $\ell > 1$NRT.

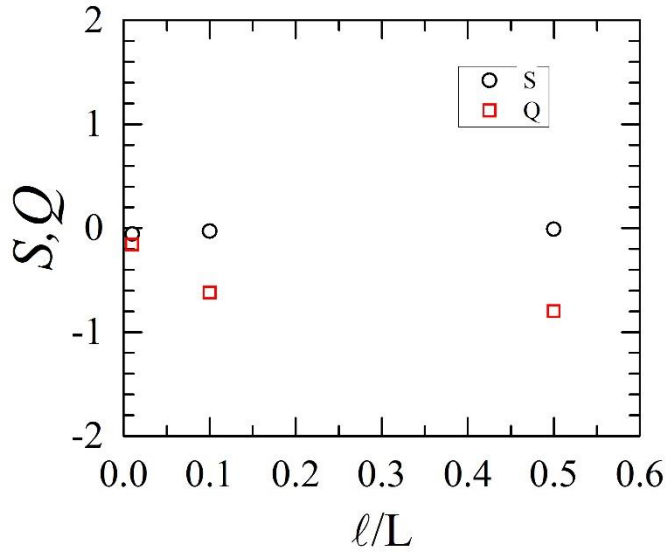

Fig. 5. 13 Plots of S and Q at the steady state for the WV model with the $\ell > 1$NRT.

does not change the up-down symmetric property and the roughness of the film surfaces of the LC and WV models. We can conclude that the $m>1$ NRT and the $\ell>1$ NRT have similar effects on the LC and WV models.

For the DT model, the $\ell>1$ NRT produces smooth morphology as shown in Fig. 3.3 (d). We found that when ℓ is increased as illustrated in Fig. 5.14 the skewness increases but the kurtosis decreases. Our result suggests $S\approx -0.3$ and $Q\approx 0.3$ at $\ell=50$. This indicates that the height distribution of the DT model nearly becomes the normal distribution at large ℓ, which is approximately consistent with the large m result.

5.3 Finite size effect on skewness and kurtosis of the height distribution at the steady state for the BD, LC, and F models.

Because the substrate size used in previous section is finite, this section shows the finite size effects on the S and Q of some growth models such as the LC, BD, and F models. Substrate size used here are $L=$ 32, 64, 128, 256, and 512. To investigate effects of the substrate size on the skewness and kurtosis, the values of these quantities are calculated from systems with different L. The obtained values, denoted S_L and Q_L are plotted as a function of $1/L^{\Delta}$, when Δ is a constant that provides the best linear fit. The curves are extrapolated back to find the values of $S_{L\to\infty}$ and $Q_{L\to\infty}$ at $1/L^{\Delta}=0$ or $L\to\infty$.

From the BD result, plots of S_L and Q_L versus $1/L^{\Delta}$ of the BD model are illustrated in Fig. 5.15. The constant Δ used here is 1. The extrapolation shows that the skewness and kurtosis are $S_{L\to\infty}=-0.22\pm0.09$ and $Q_{L\to\infty}=0.2\pm0.1$, in agreement with previous work [12].

For the LC model, we obtained the constant Δ that yields the best linear fit is 0.2 as shown in Fig. 5.16. In Fig 5.16, the data indicates that when $L\to\infty$ the skewness and kurtosis convert to $S_{L\to\infty}=0.05\pm0.02$ and $Q_{L\to\infty}=-0.62\pm0.07$.

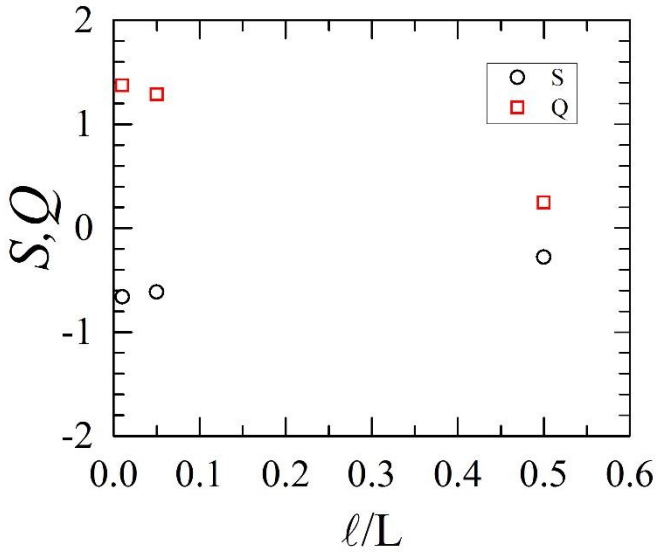

Fig. 5. 14 Plots of S and Q at the steady state for the DT model with the $\ell > 1$NRT.

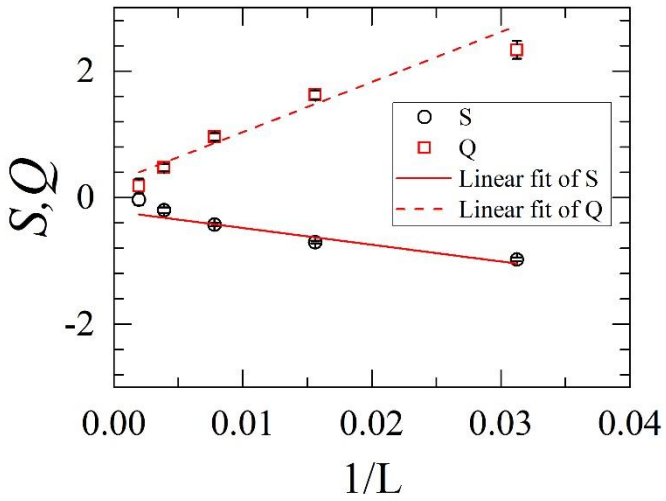

Fig. 5. 15 Plots of S and Q at the steady state versus $1/L$ of the BD model when L = 32, 64, 128, 256, and 512.

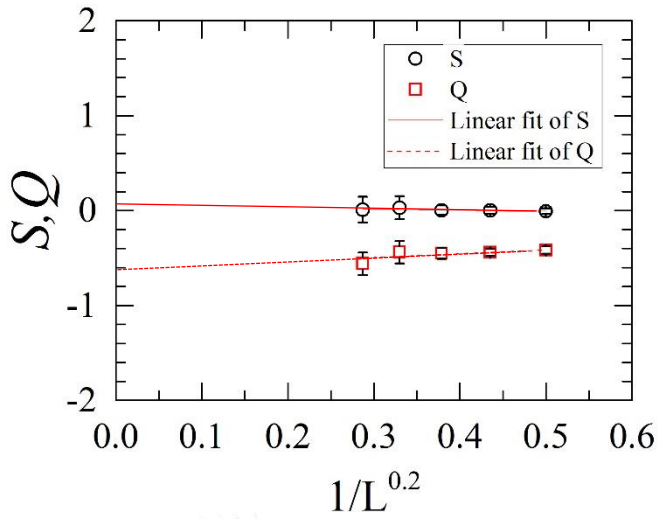

Fig. 5. 16 Plots of S and Q at the steady state versus $1/L^{0.2}$ of the LC model when L = 32, 64, 128, 256, and 512.

Comparing the noise reduced values of S and Q in Fig. 5.9 and Fig. 5.12 (using the values from the largest m and ℓ) with the $S_{L\to\infty}$ and $Q_{L\to\infty}$ from Fig. 5.16, we find them to be approximately the same. Moreover, from Fig. 5.16, it can be seen that the finite size effect on the values of S and Q is very weak in the LC model. Similar to the very weak dependent of S and Q on the noise reduction parameters m and ℓ in the previous subsection.

In the F model, plots of S_L and Q_L versus $1/L$ are presented in Fig. 5.17. The values of $S_{L\to\infty}$ and $Q_{L\to\infty}$ approximately equal -0.03. This shows that finite size substrates do not have strong effect on the height distribution of F model.

From our results, the LC and WV models with the $m>1$ and the $\ell>1$ NRTs yields a single mounded morphology. We found that S and Q do not change significantly with parameters m and ℓ. Our results show that $S\approx 0$ both in the original and the noise reduced models which confirms the up-down symmetric property of the single mounded surface of the models. Q is found to be negative which indicates that the steady state morphology of the model is rough. It is important to note that mounded and rough surfaces are indistinguishable using the value of Q.

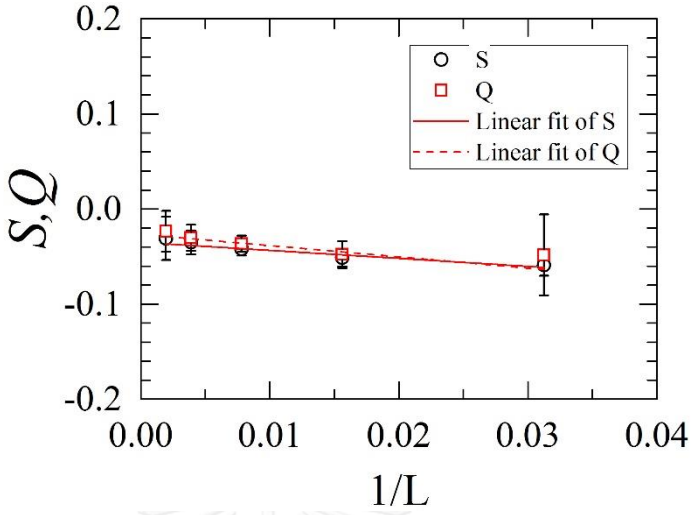

Fig. 5. 17 Plots of S and Q at the steady state versus $1/L$ of the F model when L = 32, 64, 128, 256, and 512.

For the DT with NRTs result, we found that, at the steady state, when m is increased the height distribution changes into the normal distribution indicated by the S and Q which convert to zero at large m. As the $\ell > 1$ DT result, the result is approximately agree with the $m > 1$ DT result. We found that the values of S and Q cannot be used to distinguish the mounded surface and the rough surface of the growth models. As the $\ell > 1$ DT result, the result is approximately agree with the $m > 1$ DT result. We found that the values of S and Q cannot be used to distinguish the mounded surface and the rough surface of the growth models. Furthermore, we have performed the extrapolation of the values of S and Q to that of a system with infinite substrate size in order to reduce the finite size effect.

CHAPTER VI

CONCLUSIONS

Our study is separated into three parts. In the first part, we have studied interface widths and growth exponents of the BD, DT, WV, and LC models in (2+1)-dimensional substrate systems. Then the DT, WV, and LC models with NRTS were investigated. According to the interface width results, the $m>1$ NRT can induce layer-by-layer growth at early growth time in DT, WV, and LC models whereas the $\ell>1$ NRT can only enhance the layer-by-layer growth for the DT and WV models. We do not see the layer-by-layer growth in the LC model because mound formation appears at very early time. Additionally, both the $m>1$ and $\ell>1$ NRTs are equivalent in changing the growth exponent towards the EW class. They both enhance the surface smoothness of the DT model. They are also equivalent in enhancing the mound formation in the WV and the LC models.

In the Second part, the roughness distribution curves at the steady state of the original BD, DT, WV, LC, and F models have been studied. Only the noise reduced DT, WV, and LC models were investigated. We found that both the $m>1$ and $\ell>1$ NRTs do not change the roughness distribution for the DT model. However, they totally transform the roughness distributions for the WV and LC models. When the values of m and ℓ are large enough, the roughness distributions of the WV and LC models change to the Gaussian distribution. This suggests that the roughness distribution of the mounded epitaxial growth should be the Gaussian distribution or the normal distribution. We also found that the substrate size does not have any effect on the roughness distribution curves of the DT, WV, and LC models. We note that the

advantage of the roughness distributions is clear when the study involves models with crossovers.

After that, we studied S and Q of the height distribution of the BD, DT, WV, LC, and F models in both early time and steady state regimes. Effects of the $m>1$ and $\ell>1$ NRTs on S and Q, and the surface morphology of the LC, WV, and DT models are investigated. For the $m>1$ NRT, the layer by layer growth mode is observed at the transient state as is evident from the oscillation of S and Q . The amplitude of the oscillation increases with m indicating that the more perfect layer by layer growth mode is obtained when the stronger NRTs are applied. The LC, WV and DT models with $m>1$ NRT show the same results and the same flat morphology for large m after completion of each layer. The oscillation of S and Q is, therefore, one of the characteristics of layer-by-layer growth mode of all growth models. When the $\ell>1$ NRT is applied to the system, rapidly damped oscillation of S and Q suggests that there is no layer-by-layer growth. The non-oscillating interface width and the mounded morphology (which are not shown here) support our conclusion. The $\ell>1$ NRT enhances the layer-by-layer- growth for the WV and DT models but it cannot induce the layer-by-layer growth for the LC model indicated by the non-oscillated interface width. Rapidly damped oscillations of $S(t)$ and $Q(t)$ also confirm our conclusion.

In the steady state, the LC and WV models with the $m>1$ and the $\ell>1$ NRTs are studied. We found that S and Q do not change significantly with parameters m and ℓ. This confirms the up-down symmetric property of the single mounded surface of the models. The steady state morphology of the models is rough. It is important to conclude that mounded and rough surfaces are analyzed using the value of Q.

For the DT, we found that, at the steady state, the NRTs transform the height distribution into the normal distribution indicated by the S and Q which convert to zero at large m or ℓ. For the BD model, the values of S and Q are strongly dependent on the substrate size. The finite substrate size does not strongly affect the height distribution in the steady state of the LC and F models.

From all results combined, we conclude that the NRTs cannot be used to find the asymptotic critical exponents (β, α, and z) for the models that have the mounded

morphology such as the LC and the WV models but they are appropriate for study of the roughness distribution of these models. The NRTs are suitable to determine the asymptotic critical exponents for the models that have kinetically rough surface without mound such as the DT and F models. The roughness distributions of the DT and F models with and without the NRTs are very similar so the NRTs are not needed to find the roughness distribution of these two models. For the BD model, the multiple hit NRT can be used to find both the asymptotic critical exponent and roughness distribution.

REFERENCES

[1] P.I. Tamborenea, S. Das Sarma, Surface-diffusion-driven kinetic growth on one-dimensional substrates, Physical Review E, 48 (1993) 2575-2594.
[2] S. Das Sarma, P.I. Tamborenea, A new universality class for kinetic growth: One-dimensional molecular-beam epitaxy, Phys. Rev. Lett, 66 (1991) 325.
[3] D.E. Wolf, J. Villain, Growth with Surface Diffusion, EPL (Europhysics Letters), 13 (1990) 389.
[4] F. Family, T. Vicsek, Scaling of the active zone in the Eden process on percolation networks and the ballistic deposition model, Journal of Physics A: Mathematical and General, 18 (1985) L75.
[5] F.D.A. Aarão Reis, Universality and corrections to scaling in the ballistic deposition model, Physical Review E, 63 (2001) 056116.
[6] F.D.A. Aarão Reis, Numerical study of discrete models in the class of the nonlinear molecular beam epitaxy equation, Physical Review E, 70 (2004) 031607.
[7] B.S. Costa, J.A.R. Euzébio, F.D.A. Aarão Reis, Finite-size effects on the growth models of Das Sarma and Tamborenea and Wolf and Villain, Physica A: Statistical Mechanics and its Applications, 328 (2003) 193-204.
[8] Z. Rácz, M. Plischke, Width distribution for (2+1)-dimensional growth and deposition processes, Physical Review E, 50 (1994) 3530-3537.
[9] M. Plischke, Z. Rácz, R. Zia, Width distribution of curvature-driven interfaces: A study of universality, Physical Review E, 50 (1994) 3589-3593.
[10] F.D.A. Reis, Numerical study of roughness distributions in nonlinear models of interface growth, Physical Review E, 72 (2005) 032601.
[11] F.D.A. Aarão Reis, Dynamic scaling in thin-film growth with irreversible step-edge attachment, Physical Review E, 81 (2010) 041605.
[12] T. Paiva, F.D.A. Aarão Reis, Height and roughness distributions in thin films with Kardar–Parisi–Zhang scaling, Surface Science, 601 (2007) 419-424.
[13] F. Silveira, F. Aarão Reis, Surface and bulk properties of deposits grown with a bidisperse ballistic deposition model, Physical Review E, 75 (2007) 061608.
[14] F.D.A. Aarão Reis, Roughness fluctuations, roughness exponents and the universality class of ballistic deposition, Physica A: Statistical Mechanics and its Applications, 364 (2006) 190-196.
[15] M. Kardar, G. Parisi, Y.-C. Zhang, Dynamic Scaling of Growing Interfaces, Physical Review Letters, 56 (1986) 889-892.
[16] T.J. Oliveira, F.D.A.A.o. Reis, Effects of grains' features in surface roughness scaling, Journal of Applied Physics, 101 (2007) 063507.
[17] S. Das Sarma, P.P. Chatraphorn, Z. Toroczkai, Universality class of discrete solid-on-solid limited mobility nonequilibrium growth models for kinetic surface roughening, Physical Review E, 65 (2002) 036144.
[18] P. Punyindu, S. Das Sarma, Noise reduction and universality in limited-mobility models of nonequilibrium growth, Physical Review E, 57 (1998) R4863-R4866.
[19] J. Kim, S. Das Sarma, Discrete models for conserved growth equations, Physical Review Letters, 72 (1994) 2903-2906.
[20] J. Krug, Turbulent interfaces, Physical Review Letters, 72 (1994) 2907-2910.
[21] T. Oliveira, F. Aarão Reis, Finite-size effects in roughness distribution scaling, Physical Review E, 76 (2007) 061601.

[22] A.L. Barabási, and Stanley, H. E., Fractal Concept in Surface Growth, Cambridge, England, 1995.
[23] F. Family, Scaling of rough surfaces: effects of surface diffusion, Journal of Physics A: Mathematical and General, 19 (1986) L441.
[24] V.R. Yazdanpanah, Z.M. Wang, S. Seydmohamadi, G.J. Salamo, RHEED study of GaAs(3 3 1)B surface, Journal of Crystal Growth, 277 (2005) 72-77.
[25] L. Brendel, H. Kallabis, D.E. Wolf, Layer-by-layer growth in noise-reduced growth models, Physical Review E, 58 (1998) 664-671.
[26] P. Chatraphorn, Z. Toroczkai, S. Das Sarma, Epitaxial mounding in limited-mobility models of surface growth, Physical Review B, 64 (2001) 205407.
[27] G.T. Zhipeng Xun, Kui Han, Hui Xia, Dapeng Hao, Yuling Chen, Rongji Wen, Mound morphology of the 2 + 1-dimensional Wolf–Villain model
caused by the step-edge diffusion effect, Physica A: Statistical Mechanics and its Applications, 389 (2010).
[28] S. Das Sarma, P. Punyindu, Z. Toroczkai, Non-universal mound formation in non-equilibrium surface growth, Surface Science, 457 (2000) L369-L375.
[29] J.W. Evans, P.A. Thiel, M.C. Bartelt, Morphological evolution during epitaxial thin film growth: Formation of 2D islands and 3D mounds, Surface Science Reports, 61 (2006) 1-128.
[30] X.Y. Zhang, D. Gall, Surface mound formation during epitaxial growth of CrN(001), Thin Solid Films, 518 (2010) 3813-3818.
[31] H.E. Stanley, Scaling, universality, and renormalization: Three pillars of modern critical phenomena, Reviews of Modern Physics, 71 (1999) S358-S366.
[32] A. Chame, F.D.A. Aarão Reis, Scaling of local interface width of statistical growth models, Surface Science, 553 (2004) 145-154.
[33] S. Das Sarma, S.V. Ghaisas, Solid-on-solid rules and models for nonequilibrium growth in 2+1 dimensions, Physical Review Letters, 69 (1992) 3762-3765.
[34] Z.W. Lai, S. Das Sarma, Kinetic growth with surface relaxation: Continuum versus atomistic models, Physical Review Letters, 66 (1991) 2348-2351.
[35] J. Krug, M. Plischke, M. Siegert, Surface diffusion currents and the universality classes of growth, Physical Review Letters, 70 (1993) 3271-3274.
[36] M. Siegert, Determining exponents in models of kinetic surface roughening, Physical Review E, 53 (1996) 3209-3214.
[37] A.C.L.a.P.Š. M. Kotrla, Roughness and nonlinearities in 2+1-dimensional growth models with diffusion, Europhys. Lett, 20 (1992) 25-30.
[38] P.P. Chatraphorn, S. Das Sarma, Layer-by-layer epitaxy in limited mobility nonequilibrium models of surface growth, Physical Review E, 66 (2002) 041601.
[39] a.C.P.T. K. M. Ramachandran, Mathematiccal statistics with applications, (2009).
[40] Z.-F. Huang, B.-L. Gu, Growth equations for the Wolf-Villain and Das Sarma-Tamborenea models of molecular-beam epitaxy, Physical Review E, 54 (1996) 5935-5941.

APPENDIX

VITA

Mrs. Pranee Disrattakit was born on 1 August 1978 in Chainat province, Thailand. In 2001, I received Bachelor degree of Science in Physics from Srinakharinwirot University, Thailand. In 2002, I received Graduate diploma in Teaching Major in Teaching Profession at the same University as Bachelor degree. Since 2002, I am physics teacher at Physics Department of Mahidol Wittayanusorn School, Thailand. In 2007, I received Master degree in Physics from Chulalongkorn University, Thailand.

Conference Presentation:

2012 P. Disrattakit and P. Chatraphorn. Roughness Distribution for (2+1)-dimensional growth models in the Edwards-Wilkinson universality class. Siam Physics congress 2012.

2012 P. Disrattakit and P. Chatraphorn. Roughness Distribution as a tool to identify the universality class of thin film growth models. 8th Mathematics and Physical Science Graduate Congress 2012.